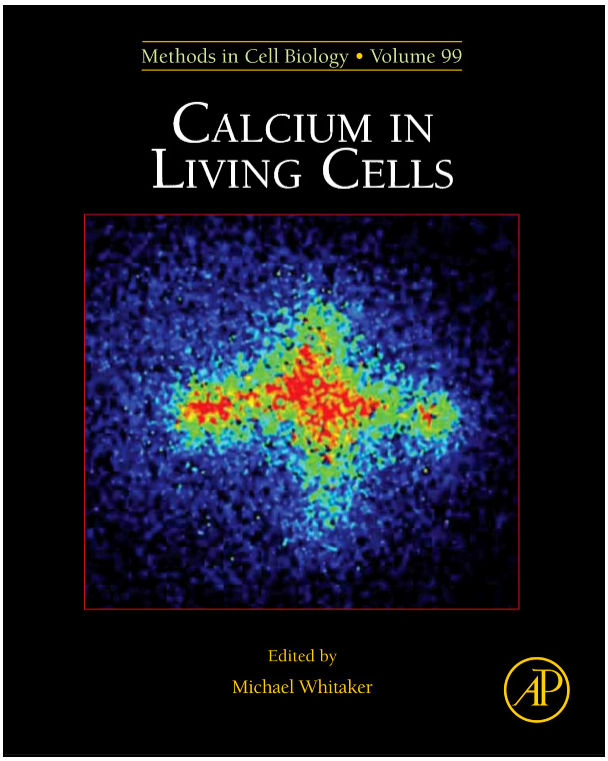

From: Robert Zucker, Photorelease Techniques for Raising or Lowering Intracellular Ca^{2+}. In Michael Whitaker, editor: Methods in Cell Biology, Vol. 99,
Burlington: Academic Press, 2010, pp. 27-66.
ISBN: 978-0-12-374841-6

CHAPTER 2

Photorelease Techniques for Raising or Lowering Intracellular Ca^{2+}

Robert Zucker

Molecular and Cell Biology Department
University of California at Berkeley
Berkeley, California, USA

METHODS IN CELL BIOLOGY, VOL. 99

0091-679X/10 $35.00
DOI: 10.1016/S0091-679X(10)99002-X

Abstract

The quantitative manipulation of intracellular calcium concentration ($[Ca^{2+}]_i$) is a valuable instrument in the modern cell biologists' toolbox for unraveling the many cell processes controlled by calcium. I summarize here the major classes of photosensitive calcium chelators used to elevate or reduce $[Ca^{2+}]_i$, with an emphasis on their physicochemical properties and methods of calculating magnitudes and kinetics of effects on $[Ca^{2+}]_i$ of flashes and steady light, in order to encourage the choice of the best substance for particular applications. The selection and calibration of appropriate light sources, and procedures for introducing the chelators into cells, spatially restricting $[Ca^{2+}]_i$ changes, and measuring the profiles of $[Ca^{2+}]_i$ changes imposed by photolysis, are also described. The final section describes a selection of biological applications.

I. Introduction

Photolabile Ca^{2+} chelators, sometimes called caged Ca^{2+} chelators, are used to control $[Ca^{2+}]_i$ in cells rapidly and quantitatively. A beam of light is aimed at cells filled with a photosensitive substance that changes its affinity for binding Ca^{2+}. Several such compounds have been invented that allow the effective manipulation of $[Ca^{2+}]_i$ in cells. These compounds offer tremendous advantages over the alternative methods of microinjecting Ca^{2+} salts, pharmacologically releasing Ca^{2+} from intracellular stores, or increasing cell membrane permeability to Ca^{2+} using ionophores, detergents, electroporation, fusion with micelles, or activation of voltage-dependent channels, in terms of specificity of action, repeatability and reliability of effect, maintenance of cellular integrity, definition of spatial extent, and rapidity of effect, all combined with the ability to maintain the $[Ca^{2+}]_i$ change for sufficient time to measure its biochemical or physiological consequences. Only photosensitive chelators allow the concentration of Ca^{2+} in the cytoplasm of intact cells to be changed rapidly by a predefined amount over a selected region or over the whole cell. Since loading can precede photolysis by a substantial amount of time, cells can recover from the adverse effects of the loading procedure before the experiments begin. The ideal photosensitive Ca^{2+} chelator does not exist, but would have the following properties.

1. The compound could be introduced easily into cell, by microinjection or by loading a membrane-permeating derivative that would be altered enzymatically to an impermeant version trapped in cells.
2. The compound could be loaded with Ca^{2+} to such a level that the unphotolyzed form would buffer the $[Ca^{2+}]_i$ to near the normal resting level, so its introduction into cells would not perturb the resting Ca^{2+} level. Additionally, by adjusting the Ca^{2+} loading or selecting chelator variants, the initial resting Ca^{2+} level could be set to somewhat higher or lower than the normal resting concentration.

3. The chelator should be chemically and photolytically stable.

4. Photolysis by a bright flash of light should allow rapid changes in the free Ca^{2+} level; this characteristic requires rapid photochemical and subsequent dark reactions of the chelator.

5. Photolysis should be achievable with biologically appropriate wavelengths, which requires a high quantum efficiency and absorbance at wavelengths that readily penetrate cytoplasm but cause little biological damage, that is, that are not highly ionizing. For the chelator to be protected from photolysis by light needed to view the preparation would also be useful.

6. The photoproducts, or postphotolysis buffer mixture, should continue to buffer Ca^{2+}, and so hold it at the new level in the face of homeostatic pressure from membrane pumps and transport processes.

7. Neither the unphotolyzed chelator nor its photoproducts should be toxic, but rather should be inert with respect to all ongoing cellular molecular and physiological processes. Three classes of compounds, the nitr series, DM-nitrophen, and the diazo series, share enough of these properties to have generated intense interest and widespread popularity, and form the subjects of this review.

Numerous more general reviews of photolabile or caged compounds, which contain some information on photolabile Ca^{2+} chelators, have appeared (Adams and Tsien, 1993; Gurney, 1993; Kao and Adams, 1993; Kaplan and Somlyo, 1989; McCray and Trentham, 1989; Ogden, 1988; Parker, 1992; Walker, 1991). Reviews focused more on photosensitive Ca^{2+} chelators may also be consulted (Ashley *et al.*, 1991a; Ellis-Davies, 2003; Gurney, 1991; Kaplan, 1990).

II. Nitr Compounds

A. Chemical Properties

The first useful class of photosensitive Ca^{2+} chelators was developed by Roger Tsien. This nitr class of compounds relies on the substitution of a photosensitive nitrobenzyl group on one or both of the aromatic rings of the Ca^{2+} chelator 1,2-bis (*o*-aminophenoxy)ethane-*N,N,N′,N′*-tetracetic acid (BAPTA) (Adams and Tsien, 1993; Adams *et al.*, 1988; Kao and Adams, 1993; Tsien and Zucker, 1986). Light absorption results in the abstraction of the benzylic hydrogen atom by the excited nitro group and oxidation of the alcohol group to a ketone. The resulting nitrosobenzoyl group is strongly electron withdrawing, reducing the electron density around the metal-coordinating nitrogens and reducing the affinity of the tetracarboxylate chelator for Ca^{2+}. In the first member of this series, nitr-2, methanol is formed as a by-product of photolysis, but in subsequent members (nitr-5, nitr-7, and nitr-8) only water is produced. Photolysis of nitr-2 is also slow (200 ms time constant). For the other nitr chelators, the dominant photolysis pathway is much faster (nitr-7, 1.8 ms; nitr-5, 0.27 ms; and nitr-8, not reported). For these reasons,

nitr-2 is no longer used. For the three remaining nitr compounds, photolysis is most efficient at the absorbance maximum for the nitrobenzhydrol group, about 360 nm, although light between 330 and 380 nm is nearly as effective. The quantum efficiency of the Ca^{2+}-bound form is about 1/25 (nitr-5, 0.035 and nitr-7, 0.042) and is somewhat less in the Ca^{2+}-free form (0.012 and 0.011). The absorbance at this wavelength is 5500 M^{-1} cm^{-1} (decadic molar extinction coefficient) for nitr-5 and nitr-7, and 11,000 M^{-1} cm^{-1} for nitr-8. The structures of the nitr series of compounds are given in Fig. 1; and the photochemical reaction of the most popular member of this group, nitr-5, is shown in Fig. 2. The physico-chemical properties of these and other photosensitive chelators are summarized in Table I.

These chelators share the advantages of the parent BAPTA chelator: high specificity for Ca^{2+} over H^+ and Mg^{2+} (Mg^{2+} affinities, 5–8 mM), lack of dependence of Ca^{2+} affinity on pH near pH 7, and fast buffering kinetics. One limitation is that the drop in affinity in the nitr compounds after photolysis is relatively modest, about 40-fold for nitr-5 and nitr-7. The Ca^{2+} affinity of nitr-5 drops from 0.15 to 6 μM at 120-mM ionic strength after complete photolysis. These affinities must be reduced at higher ionic strength, roughly in proportion to the tonicity (Tsien and Zucker, 1986). By incorporating a *cis*-cyclopentane ring into the bridge between the chelating ether oxygens of BAPTA, nitr-7 was created

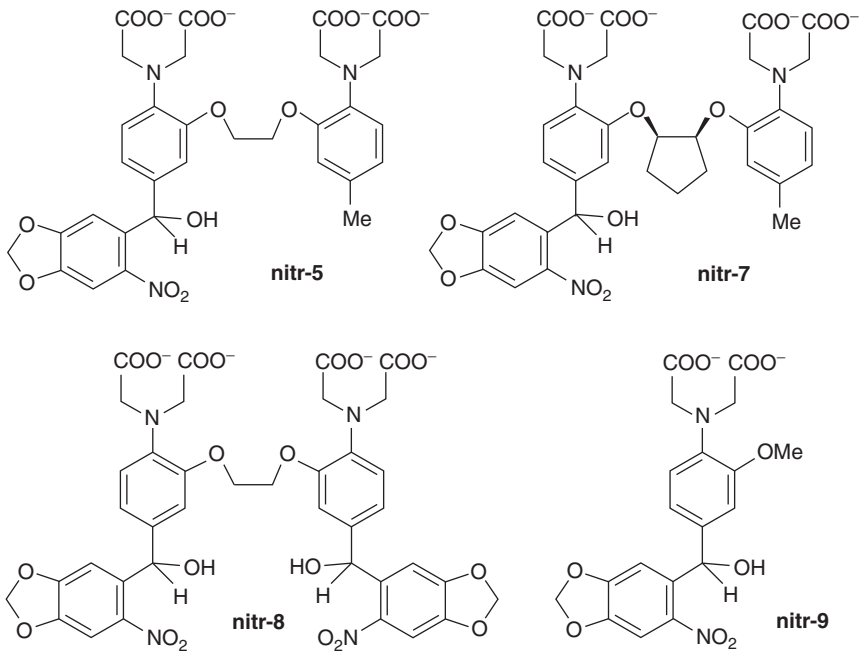

Fig. 1 Structures of the nitr series of photolabile chelators, which release calcium on exposure to light.

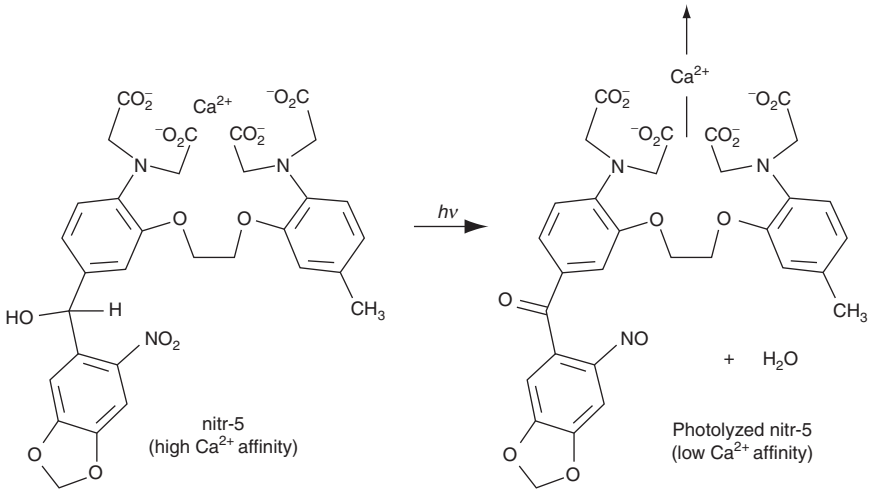

Fig. 2 Reaction scheme for the photorelease of nitr-5.

with significantly higher Ca^{2+} affinities (54 nM, decreasing to 3 μM after photolysis at 120 mM ionic strength). To increase the change in Ca^{2+}-binding affinity on photolysis, nitr-8 was created with a 2-nitrobenzyl group on each aromatic ring of BAPTA. Photolysis of each group reduces affinity only about 40-fold, as for nitr-5 and nitr-7, but photolysis of both nitrobenzyl groups reduces affinity nearly 3000-fold, to 1.37 mM, with a quantum efficiency of 0.026. Finally, nitr-9 is a dicarboxylate 2-nitrobenzhydrol with a low Ca^{2+} affinity that is unaffected by photolysis; this compound can be used to control for nonspecific effects of the photoproducts.

Initially, nitr-5 was the substance most often applied in biological experiments, largely because it was the first photolabile chelator to have most of the qualities of the ideal substance. The limited affinity for Ca^{2+} of this substance in the unphotolyzed form requires that it be lightly loaded with Ca^{2+} when introduced into cells; otherwise, the resting $[Ca^{2+}]_i$ will be too high. However, the compound in a lightly loaded state contains little Ca^{2+} to be released on photolysis. Nitr-7 alleviates this problem with an affinity closer to that of normal resting $[Ca^{2+}]_i$, but its synthesis is more difficult and its photochemical kinetics are significantly slower. Both compounds permit less than two orders of magnitude increase in $[Ca^{2+}]_i$, generally to only the low micromolar range, and then only with very bright flashes or prolonged exposures to steady light to achieve complete photolysis. Nitr-8 permits a much larger change in $[Ca^{2+}]_i$. Photolysis kinetics for this compound have not yet been reported. Neither nitr-8 nor the control compound nitr-9 is presently commercially available; nitr-5 and nitr-7 are supplied by CalBiochem (La Jolla, California).

Table I
Properties of photosensitive Ca chelators

Compound (availability)	τ_{Phot} (ms)	λ_{max} (nm)	Q.E.$_{Ca}$	Q.E.$_{free}$	Before photolysis		After photolysis		Before photolysis		After photolysis		Ca-binding on-rate
					$K_{D\text{-}Ca}$ (μM)	$K_{D\text{-}Mg}$ (mM)	$K_{D\text{-}Ca}$ (μM)	$K_{D\text{-}Mg}$ (mM)	$\varepsilon_{10\text{-}Ca}$ (M^{-1} cm^{-1})	$\varepsilon_{10\text{-}free}$ (M^{-1} cm^{-1})	$\varepsilon_{10\text{-}Ca}$ (M^{-1} cm^{-1})	$\varepsilon_{10\text{-}free}$ (M^{-1} cm^{-1})	
Nitr-5	0.27	365	0.035	0.012	0.145	8.5	6.3	8	5450	5750	13,800	27,300	0.5
Nitr-7	1.8	365	0.042	0.011	0.054	5.4	3.0	5	5780	5540	24,700	10,000	0.2
Nitr-8	–	365	0.026[b]	–	0.5	–	1370	–	11,000	1100	~50,000	~20,000	–
Nitr-9	–	365	~0.02	~0.02	~1000	~10	~1000	~10	~5500	~5500	~15,000	~25,000	–
Azid-1	<2.0	342	1.0	0.9	0.23	8	120	8	33,000	27,000	11,500	5550	0.8
DM-nitrophen	0.015;1.9	370	0.18	0.18	0.007[c]	0.0017[c]	4200;89	2.5	4330	4020	3150	3150	0.02
NP-EGTA	0.002	345	0.23	0.23	0.08[c]	9	1000	9	975	975	1900	1900	0.017
DMNPE-4	–	347	0.09	0.09	0.048[d]	7	1000	7	5140	5140?	5140?	5140?	0.01?
NDBF-EGTA	0.01;0.52	330	0.7	0.7	0.1	15	1000	15	18,400	18,400?	18,400?	18,400?	–
Diazo-2	0.134	370	0.057[a]	0.030[a]	2.2	5.5	0.073	3.4	2080	22,200	700	2080	0.8
Diazo-4	–	370	0.030[a,b]	0.030[a,b]	89	–	0.055	2.6	4600	46,000	<500	<500	0.8
Diazo-3	0.24	375	0.048	0.048	>1000	20	>1000	20	2100	22,800	700	2100	0.8

τ_{Phot}, photolysis time constant; λ_{max}, absorbance maximum of Ca-loaded compound; most effective photolysis wavelength; Q.E.$_{Ca,free}$, quantum efficiency, Ca-bound (free); $K_{D\text{-}Ca,Mg}$, Ca (Mg) dissociation constant (1/affinity) at 0.1–0.15 M ionic strength; and $\varepsilon_{10\text{-}Ca,free}$, decadic absorbance extinction coefficient of Ca-bound (free) compound.

[a]10% of absorbed photons produce a nonphotolyzable photoproduct similar in absorbance and affinities to unphotolyzed diazo.

[b]For photolysis of each site.

[c]At pH 7.2; doubles for each 0.3 pH unit reduction.

[d]At pH 7.2; increases 2.5× for each 0.2 pH unit reduction.

The latest addition to the nitr-like class of compounds based on BAPTA is Azid-1 (Adams *et al.*, 1997). This compound was derived from the high-affinity fluorescent indicator derivative of BAPTA, fura-2, by addition of an azido substituent to fura's benzofuran-3 position. Unlike fura-2, neither this compound nor its photoproducts are fluorescent; and unlike the other nitr compounds and the dimethoxynitrophenyl class of Ca^{2+} chelators (see below), it relies on the photosensitivity of an aromatic azide rather than a nitrobenzyl group. UV absorption peaking at 372 nm (342 nm for the Ca^{2+}-bound form) probably leads to formation of a nitrene which steals hydrogen from water to produce an amidine, which with another hydrogen converts to a nitrenium that rapidly combines with water to form an amidinium that reacts with OH^- to produce the final low-affinity electron-withdrawing benzofurane-3-one photoproduct plus ammonia. Thus, photolysis absorbs one net proton and produces one molecule of ammonia for each molecule of azid-1 photolyzed, which can lead to an elevation of pH_i in weakly buffered cells.

This disadvantage is counterbalanced by substantial advantages. Photolysis of both Ca^{2+}-bound and Ca^{2+}-free forms of zaid-1 is phenomenally efficient (Q.E. ≈ 1), and azid-1 is very UV-dark, absorbing at 33,000 $M^{-1}\,cm^{-1}$ when Ca^{2+}-bound (or 27,000 $M^{-1}\,cm^{-1}$ when free); these factors combine to make it 250–300 times more sensitive to light than nitr-5! Moreover, its Ca^{2+}-affinity drops from 230 nM to 120 μM, on photolysis, a change that is 12 times the change in nitr-5 affinity on photolysis. Like the nitr compounds, it hardly binds Mg^{2+} at all ($K_D = 8$ mM), and its Ca^{2+}-binding ($\sim 10^9\ M^{-1}\ s^{-1}$) and photolysis rates ($\tau < 2\ \mu s$) are equally rapid. In most respects, azid-1 comes closest to the ideal-caged Ca^{2+} compound. Unfortunately, its synthesis is quite difficult, and it has never been commercially available; at present, apparently none exists at all.

B. Calculating $[Ca^{2+}]_i$ Changes in Cells

If nitr-5 or azid-1 is photolyzed partially by a flash of light, the reduction in Ca^{2+} affinity of a portion of the chelator occurs within $\sim$0.3 ms. During this period of photolysis, low-affinity buffer is being formed and high-affinity buffer is vanishing while the total amount of Ca^{2+} remains unchanged. As the buffer concentrations change, Ca^{2+} ions reequilibrate among the new buffer concentrations by shifting from the newly formed low-affinity photoproduct to the remaining unphotolyzed high-affinity caging chelator. Since the on-rate of binding is close to the diffusion limit (as calculated from Adams *et al.*, 1988; see also Ashley *et al.*, 1991b), this equilibration occurs much faster than photolysis, and Ca^{2+} remains in quasi-equilibrium throughout the photolysis period. The $[Ca^{2+}]_i$ in a cell rises smoothly in a step-like fashion over a period of 0.3 ms from the low level determined by the initial concentrations of total Ca^{2+}, and unphotolyzed chelator to a higher level determined by the final concentrations of all the chelator species after partial photolysis. At least in the case of nitr-5, $[Ca^{2+}]_i$ remains under the control of the low- and high-affinity species, so the elevated Ca^{2+} is removed only gradually by extrusion and uptake into organelles. Thus, nitr-5 and azid-1 are well suited to

producing a modest but quantifiable step-like rise in response to a partially photolyzing light flash, or a gradually increasing $[Ca^{2+}]_i$ during exposure to steady light. Subsequent flashes cause further increments in $[Ca^{2+}]_i$. These increments actually increase because, with each successive flash, the remaining unphotolyzed chelator is loaded more heavily with Ca^{2+}. Eventually, unphotolyzed nitr-5 or azid-1 is fully Ca^{2+}-bound, and subsequent flashes elevate Ca^{2+} by smaller increments as the amount of unphotolyzed chelator drops.

If a calibrated light source is used that photolyzes a known fraction of nitr in the light path, or in cells filled with chelator and exposed either fully or partially to light, then the mixture of unphotolyzed nitr and photoproducts may be calculated with each flash (Landò and Zucker, 1994; Lea and Ashley, 1990). The different quantum efficiencies of free and Ca^{2+}-bound chelators must be taken into account. Simultaneous solution of the buffer equations for photolyzed and unphotolyzed chelators and native Ca^{2+} buffers predicts the $[Ca^{2+}]_i$. For sufficiently high nitr-5 concentration (above 5 mM), the native buffers have little effect and usually may be ignored in the calculation. Further, since $[Ca^{2+}]_i$ depends on the proportion of chelator loaded with Ca^{2+}, the exact chelator concentration in the cell makes little difference, at least in small cells or cell processes.

If the cell is large, the light intensity will drop as it passes from the front to the rear of the cell. Knowing the absorbance of cytoplasm and chelator species at 360 nm, and the chelator concentration before a flash, the light intensity and photolysis rate at any point in the cytoplasm may be calculated. A complication in this calculation is that nitr-5 photoproducts have very high absorbance (Ca^{2+}-free photoproduct, 24,000 $M^{-1}\,cm^{-1}$ and Ca^{2+}-bound photoproduct, 10,000 $M^{-1}\,cm^{-1}$) (Adams *et al.*, 1988). As photolysis proceeds, the cell darkens and photolysis efficiency is reduced by self-screening. For azid-1 the situation is reversed: its photoproducts have much lower absorbance (11,500 and 5000 $M^{-1}\,cm^{-1}$) for Ca^{2+}-bound and free species or 1/3 and 1/4 of the respective unphotolyzed forms. Thus light penetrates more deeply as photolysis proceeds. Regardless, with estimation of the spatial distribution of light intensity from Beer's Law, the spatial concentrations of photolyzed and unphotolyzed chelator can be computed; from this calculation follows the distribution of the rise in $[Ca^{2+}]_i$. The subsequent spatial equilibration of $[Ca^{2+}]_i$ can be calculated by solving diffusion equations, often in only one dimension, using the initial $[Ca^{2+}]_i$ and chelator distributions as the boundary conditions. Effects of endogenous buffers, uptake, and extrusion mechanisms on the rise in $[Ca^{2+}]_i$ can be incorporated into the calculations. Simulations of the temporal and spatial distribution of $[Ca^{2+}]_i$ have been devised (Zucker, 1989) and applied to experimental data on physiological effects of $[Ca^{2+}]_i$; the predicted changes in $[Ca^{2+}]_i$ have been confirmed with Ca^{2+}-sensitive dyes (Landò and Zucker, 1989). Simplified and approximate models using the volume-average light intensity to calculate volume-average photolysis rate and average $[Ca^{2+}]_i$ changes often suffice when the spatial distribution of $[Ca^{2+}]_i$ is not important, for example, in small cells or processes or when estimating the change in $[Ca^{2+}]_i$ in a cell after diffusional equilibration has occurred.

III. DM-Nitrophen

A. Chemical Properties

Graham Ellis-Davies followed a different strategy for releasing Ca^{2+}—by attaching a 2-nitrobenzyl group to one of the chelating amines of ethylenediaminetetraacetic acid (EDTA) to form the photosensitive chelator dimethoxynitrophenyl-EDTA or DM-nitrophen (Ellis-Davies and Kaplan, 1988; Kaplan and Ellis-Davies, 1988). Photolysis by UV light in the wavelength range 330–380 nm cleaves the DM-nitrophen with a quantum efficiency of 0.18 through multiple intermediate pathways (McCray *et al.*, 1992) to form iminodiacetic acid and a H^+-absorbing 2-nitrosoacetophenone derivative, with 65% of the photoproducts formed with a time constant of 15 μs and the rest with $\tau = 1.9$ ms (Faas *et al.*, 2005, 2007). A simplified reaction is shown in Fig. 3. Although DM-nitrophen binds Ca^{2+} with an affinity of 7 nM at pH 7.2, Ca^{2+}-bound chelator forms a photoproduct-binding Ca^{2+} with a 4-mM affinity, while the free form (and Mg^{2+}-bound forms, see below) photolyze to a 90 μM-K_D photoproduct at an ionic strength of 150 mM. These values are from the most recent of the continually evolving models of DM-nitropen photolysis (Ayer and Zucker, 1999; Bollmann and Sakmann, 2005; Faas *et al.*, 2005, 2007; Kaplan and Ellis-Davies, 1988; Neher and Zucker, 1993). Thus, complete photolysis of Ca^{2+}-DM-nitrophen can elevate Ca^{2+} over 50,000-fold, much more than photolysis of the nitr compounds or azid-1. This significant advantage is counterbalanced to some extent by the facts that the photoproducts buffer Ca^{2+} so weakly that the final $[Ca^{2+}]_i$ will be determined largely by native cytoplasmic buffers, and that the Ca^{2+} liberated by photolysis of DM-nitrophen will be removed more readily by extrusion and uptake pumps.

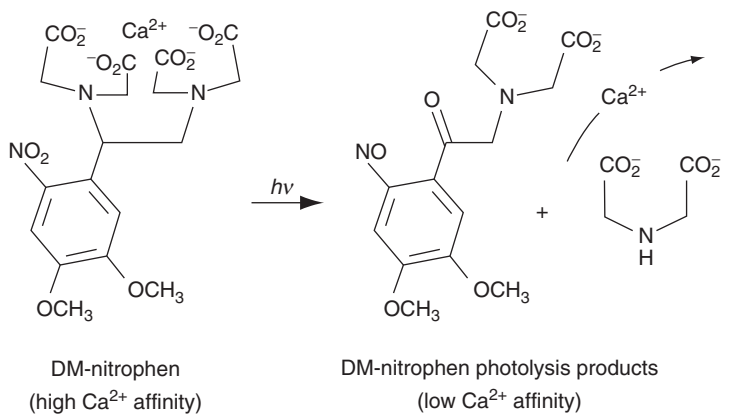

Fig. 3 Structure of and reaction scheme for DM-nitrophen, which releases calcium on exposure to light.

The absorbance of Ca^{2+}-saturated and free DM-nitrophen is 4330 and 4020 M^{-1} cm^{-1}, respectively, and 0.18.

A serious complication of DM-nitrophen is that it shares the cation-binding properties of its parent molecule EDTA. In particular, H^+ and Mg^{2+} compete for Ca^{2+} at the hexacoordinate-binding site. The affinity of DM-nitrophen for Mg^{2+} at pH 7.2 is 1.7 μM, whereas the photoproducts bind Mg^{2+} with affinities of about 2 mM. Further, both the Ca^{2+}- and Mg^{2+}-affinities of DM-nitrophen are highly pH-dependent (Grell *et al.*, 1989), doubling for each 0.3 units of pH increase. Thus, in the presence of typical $[Mg^{2+}]_i$ levels of 1–3 mM, DM-nitrophen that is not already bound to Ca^{2+} will be largely in the Mg^{2+}-bound form. Further, excess DM-nitrophen will suck Mg^{2+} off ATP, which binds it substantially more weakly, compromising the ability of ATP to serve as an energy source or as a substrate for ATPases. Finally, photolysis of DM-nitrophen will lead to a jump in $[Mg^{2+}]_i$ as well as $[Ca^{2+}]_i$, and to a rise in pH. Unless controlled by native or exogenous pH buffers, this pH change can alter the Ca^{2+} and Mg^{2+} affinities of the remaining DM-nitrophen. In the absence of Ca^{2+}-loading, DM-nitrophen even may be used as a caged Mg^{2+} chelator (Ellis-Davies, 2006). Attributing physiological responses to a $[Ca^{2+}]_i$ jump, therefore, requires control experiments in which DM-nitrophen is not charged with Ca^{2+}. DM-nitrophen currently is sold by CalBiochem.

To circumvent the problems arising from Mg^{2+} competing for the Ca^{2+}-binding site of DM-nitrophen, a second generation derivative of ethylene glycol bis(β-aminoethylether)-*N,N,N′,N′*-tetraacetic acid (EGTA, which binds Mg^{2+} only very weakly) coupled to a light-sensitive *ortho*-nitrophenyl group was developed (Ellis-Davies and Kaplan, 1994). This compound, nitrophenyl-EGTA or NP-EGTA, is very rapidly cleaved ($\tau = 2$ μs) (Ellis-Davies, 2003) to H^+-absorbing imidodiacetic acid photoproducts with effective Ca^{2+}-K_D of 1 mM, 12,500-fold higher (lower affinity) than that of the unphotolyzed cage (80 nM) at pH 7.2, with pH-dependence similar to that of EGTA, EDTA, and DM-nitrophen. Unlike DM-nitrophen, Mg^{2+} binding to NP-EGTA is negligible (9 mM before and after photolysis). Quantum efficiency (0.23) is similar to that of DM-nitrophen, and higher than for the nitr compounds, but less than that of azid-1. However, photolysis efficiency is seriously limited by its low absorbance (975 M^{-1} cm^{-1}), only 1/6—1/4 those of the nitr compounds and DM-nitrophen, and less than 3% of azid-1's absorbance.

More recently, a dimethoxy-*ortho*-nitrophenyl derivative of EGTA (DMNPE-4) was introduced (Ellis-Davies and Barsotti, 2006), with somewhat higher Ca^{2+} affinity (48 nM), dropping with time constants of 10 and 17 μs to 1 mM on photolysis, low Mg^{2+}-affinity (7 mM), and under half the quantum efficiency (0.09) but over five times the absorbance (5140 $M^{-1}cm^{-1}$), thus twice the photolysis efficiency of NP-EGTA. An additional very slow phase releasing 30% of caged Ca^{2+} with $\tau \approx 667$ ms was observed.

Ellis-Davies' lab has also produced a new generation of EGTA-based chelators using the novel photosensitive chromophore nitrodibenzofuran or NDBF-EGTA (Momotake *et al.*, 2006). This compound binds Ca^{2+} with $K_D = 100$ nM at pH 7.2,

presumably with an on-rate similar to that of the other EGTA derivatives. Ca^{2+} affinity drops sharply to $\sim$1 mM on photolysis with time constants of 14 and 520 μs. Quantum efficiency (0.7) and absorbance (18,400 M^{-1} cm^{-1}) are extremely high, as is the change in Ca^{2+} affinity (10,000-fold at pH 7.2), making this a very attractive candidate for future-caged Ca^{2+} research.

B. Calculating Changes in $[Ca^{2+}]_i$

Calculating $[Ca^{2+}]_i$ changes on photolysis of NP-EGTA and its congeners is similar to that for the nitr compounds (if the pH dependence of binding constants is ignored), since Mg^{2+} binding is not an issue. Since the chelators' Ca^{2+} affinities is similar to resting cytoplasmic $[Ca^{2+}]_i$ levels, filling cells with a half-Ca^{2+}-loaded chelator will not disturb $[Ca^{2+}]_i$ but can release substantial amounts of Ca^{2+} ($\sim$1 mM) which will be reduced about 100-fold by the cell's endogenous buffers. However, except for NDBF-EGTA, the low absorbance usually limits flash photolysis to at most about 20%.

Quantifying changes in $[Ca^{2+}]_i$ caused by photolysis is much more difficult for DM-nitrophen. The initial level of $[Ca^{2+}]_i$ before photolysis depends upon the total concentrations of Mg^{2+}, Ca^{2+}, DM-nitrophen, ATP, and native Ca^{2+} buffers, because at least two buffers (DM-nitrophen and endogenous buffers) compete for Ca^{2+}, two buffers (ATP and DM-nitrophen) compete for Mg^{2+}, and, after partial photolysis, both cations also bind to the two photoproducts. Calculating equilibrium Ca^{2+} levels involves simultaneous solution of at least six nonlinear buffer equations (Delaney and Zucker, 1990), which is a tedious chore at best. Also, the various dissociation constants depend on ionic strength, and have been measured only at 150 mM. The high affinity of DM-nitrophen for Ca^{2+} might appear to dominate the buffering of Ca^{2+} in cytoplasm, but this idea is misleading. A solution of DM-nitrophen that is 50% saturated with Ca^{2+} will hold the free $[Ca^{2+}]_i$ at 7 nM at pH 7.2; this action will be independent of the total DM-nitrophen concentration. However, 5 mM DM-nitrophen with 2.5 mM Ca^{2+} and 5 mM Mg^{2+} will buffer free $[Ca^{2+}]_i$ to about 2 μM; now doubling all concentrations results in a final $[Ca^{2+}]_i$ of around 5 μM. Since the total $[Mg^{2+}]_i$ available, as free or weakly bound to ATP, is several millimolar, partially Ca^{2+}-loaded DM-nitrophen may bring the resting Ca^{2+} level to a surprisingly high level. Because the solution is still buffered, this $[Ca^{2+}]$ may be reduced only gradually by pumps and uptake, but eventually Ca^{2+} will be pumped off the DM-nitrophen until the $[Ca^{2+}]_i$ is restored to its normal level. Then photolysis may lead to only tiny jumps in $[Ca^{2+}]_i$. However, if a large amount of Ca^{2+}-loaded-DM-nitrophen is introduced into a cell relative to the total $[Mg^{2+}]_i$, Ca^{2+} can be buffered to low levels while photolysis can release a large amount. In fact, if enough DM-nitrophen is introduced into cells with no added Ca^{2+}, it may gradually absorb Ca^{2+} from cytoplasm and intracellular stores and photolysis can produce a substantial jump in $[Ca^{2+}]_i$. Therefore, both resting and the postphotolysis levels of Ca^{2+} may vary over very wide ranges, depending on $[DM\text{-}nitrophen]_i$, $[Mg^{2+}]_i$, and cellular $[Ca^{2+}]_i$ control

processes, all of which are difficult to estimate or control. Thus, quantification of changes in $[Ca^{2+}]_i$ is not easy to achieve.

The situation may be simplified by perfusing cells with Ca^{2+}-DM-nitrophen solutions while dialyzing out Mg^{2+} and mobiles endogenous buffers (Neher and Zucker, 1993; Thomas *et al.*, 1993). Of course, this procedure will not work in studies of cell processes requiring Mg^{2+}-ATP or if perfusion through whole-cell patch pipettes is not possible.

Another consequence of Mg^{2+} binding by DM-nitrophen is that cytoplasmic Mg^{2+} may displace Ca^{2+} from DM-nitrophen early in the injection or perfusion procedure, leading to a transient rise in $[Ca^{2+}]_i$ before sufficient DM-nitrophen is introduced into the cell (Neher and Zucker, 1993; Parsons *et al.*, 1996; Thomas *et al.*, 1993). Such a "loading transient" was accurately predicted from models of changes of the concentrations of total $[Ca^{2+}]_i$, $[Mg^{2+}]_i$, ATP, native buffer, and DM-nitrophen during filling from a whole-cell patch electrode (R. S. Zucker, unpublished). Since this process may have important physiological consequences, controlling it is important. The process may be eliminated largely by separating the Ca^{2+}-DM-nitrophen-filling solution in the pipette from the cytoplasm by an intermediate column of neutral solution [such as dilute EGTA or BAPTA] in the tip of the pipette, which allows most of the Mg^{2+} to escape from the cell before the DM-nitrophen begins to enter. Then most of the loading transient occurs within the tip of the pipette.

One method of better controlling the change in $[Ca^{2+}]_i$ in DM-nitrophen experiments is to fill cells with a mixture of Ca^{2+}-DM-nitrophen and another weak Ca^{2+} buffer such as *N*-hydroxyethylethylenediaminetriacetic acid (HEEDTA) or 1,3-diaminopropan-2-ol-tetraacetic acid (DPTA) (Neher and Zucker, 1993). These tetracarboxylate Ca^{2+} chelators have Ca^{2+} affinities in the micromolar or tens of micromolar range. If cells are filled with such a mixture without Mg^{2+}, the initial Ca^{2+} level can be set by saturating the DM-nitrophen and adding appropriate Ca^{2+} to the other buffer. Then photolysis of DM-nitrophen releases its Ca^{2+} onto the other buffer; the final Ca^{2+} can be calculated from the final buffer mixture in the same fashion as for the nitr compounds. Since all the constituent affinities are highly pH dependent, a large amount of pH buffer (e.g., 100 mM) should be included in the perfusion solution, and the pH of the final solution adjusted carefully.

The kinetic behavior of DM-nitrophen and the NP-EGTAs is much more complex than their equilibrium reactions. Photolysis proceeds rapidly ($\tau s = 0.2$ and 2 ms for DM-nitrophen, 2 μs for NP-EGTA), but the on-rate of Ca^{2+} binding is much slower, about 20 mM^{-1} ms^{-1} (Ellis-Davies, 2003; Faas *et al.*, 2005, 2007). This characteristic has particularly interesting consequences for partial photolysis of partially Ca^{2+}-loaded chelator. A flash of light will release some Ca^{2+}, which initially will be totally free. If the remaining unphotolyzed and unbound chelator concentration exceeds that of the released Ca^{2+}, this Ca^{2+} will rebind, displacing H^+ within milliseconds and producing a brief $[Ca^{2+}]_i$ "spike" (Ellis-Davies *et al.*, 1996; Grell *et al.*, 1989; Kaplan, 1990; McCray *et al.*, 1992), followed by a near-step

fall in pH. If Mg^{2+} is also present, a secondary relaxation of $[Ca^{2+}]_i$ follows because of the slower displacement of Mg^{2+} from DM-nitrophen (Ayer and Zucker, 1999; Delaney and Zucker, 1990; Escobar *et al.*, 1995, 1997). Moreover, if a steady UV source is used to photolyze DM-nitrophen, rebinding continually lags release, leading to a low (micromolar range) free $[Ca^{2+}]_i$ while the illumination persists. When the light is extinguished, the $[Ca^{2+}]_i$ drops rapidly to a low level under control of the remaining chelator (Zucker, 1993). In the case of DM-nitrophen bound to Mg^{2+}, achievement of equilibrium is somewhat slower (tens of milliseconds). Thus, a reversible "pulse" of $[Ca^{2+}]_i$ is generated, the amplitude of which depends on light intensity and the duration of which is controlled by the length of the illumination. This situation remains so until the remaining unphotolyzed cage becomes fully saturated with Ca^{2+}, whereupon $[Ca^{2+}]_i$ escapes from the control of the chelator, imposing a practical limit on the product of $[Ca^{2+}]_i$ and duration of about 0.75 μM s for DM-nitrophen. Similar kinetic considerations apply when Ca^{2+} is passed by photolysis from a Ca^{2+} cage to another buffer such as BAPTA, EGTA, HEEDTA, or DPTA. Judicious selection of buffers and buffer ratios may be used to shape this Ca^{2+} "spike" to match a hypothetical naturally occurring $[Ca^{2+}]_i(t)$ waveform and test its physiological consequences (Bollmann and Sakmann, 2005). If this behavior is considered undesirable, it may be avoided by using only fully Ca^{2+}-saturated DM-nitrophen, due to its extremely high Ca^{2+}-affinity, for which rebinding to unphotolyzed chelator is impossible. Thus, the kinetic complexity of the nitrophen class of chelators can be turned to experimental advantage, greatly magnifying the flexibility of experimental $[Ca^{2+}]_i$ control.

IV. Diazo Compounds

A. Chemical Properties

In some experiments, being able to lower the $[Ca^{2+}]_i$ rapidly, rather than raise it, is desirable. For this purpose, caged chelators were developed. Initial attempts involved attachment of a variety of photosensitive protecting groups to mask one of the carboxyl groups of BAPTA, thus reducing its Ca^{2+} affinity until restored by photolysis. Such compounds displayed low quantum efficiency (Adams *et al.*, 1989; Ferenczi *et al.*, 1989) and their development has not been pursued. A more successful approach (Adams *et al.*, 1989) involved substituting one (diazo-2) or both (diazo-4) of the aromatic rings of BAPTA with an electron-withdrawing diazoketone that reduces Ca^{2+} affinity, much like the photoproducts of the nitr compounds. Figure 4 shows the structures of the diazo series of chelators. Photolysis converts the substituent to an electron-donating carboxymethyl group while releasing a proton; the Ca^{2+} affinity of the photoproduct is thereby increased. The reaction is illustrated in Fig. 5.

Diazo-2 absorbs one photon with quantum efficiency 0.03 to increase affinity, in 433 μs, from 2.2 μM to 73 nM at 120-mM ionic strength (or to 150 nM at 250 mM

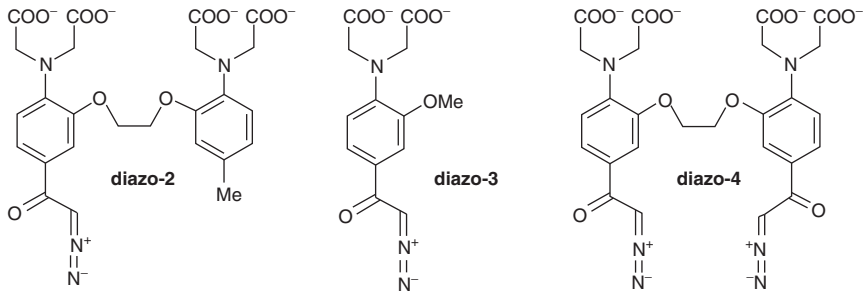

Fig. 4 Structures of the diazo series of photolabile chelators, which take up calcium on exposure to light.

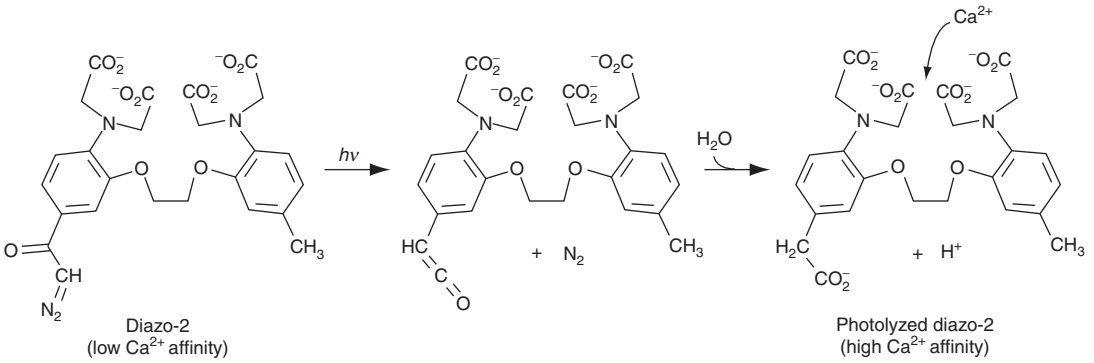

Fig. 5 Reaction scheme for the photolysis of diazo-2.

ionic strength). The absorbance maximum of the photosensitive group is 22,200 $M^{-1}\,cm^{-1}$ at 370 nm, and drops to negligible levels at this wavelength after photolysis. A small remaining absorbance reflects formation of a side product of unenhanced affinity and unchanged molar extinction coefficient in 10% of the instances of effective photon absorption. This ''inactivated'' diazo still binds Ca^{2+} (with some reduction in absorbance), but is incapable of further photolysis. The Ca^{2+}-bound form of diazo-2 has about one-tenth the absorbance of the free form, dropping to negligible levels after photolysis, with quantum efficiency of 0.057 and a time constant of 134 μs. Binding of Ca^{2+} to photolyzed diazo-2 is fast, with an on-rate of $8 \times 10^8\ M^{-1}\,s^{-1}$. Mg^{2+} binding is weak, dropping from 5.5 to 3.4 mM after photolysis, and pH interference is small with this class of compound.

One limitation of diazo-2 is that the unphotolyzed chelator has sufficient Ca^{2+} affinity that its incorporation into cytoplasm is likely to reduce resting levels to some degree, and certainly will have some effect on $[Ca^{2+}]_i$ rises that occur physiologically. To obviate this problem, diazo-4 was developed with two

photolyzable diazoketones. Absorption of one photon increases the Ca^{2+} affinity from 89 to 2.2 μM (with a 10% probability of producing a side-product with one inactivated group). Absorption of two photons (with a probability assumed to equal the square of the probability of one group absorbing one photon, and with a measured quantum efficiency of 0.015) results in further increase of the affinity to 55 nM, a total increase of 1600-fold. This large increase in affinity is, to some extent, offset by the small fraction of diazo-4 that can be doubly photolyzed readily. Thus, a flash of light produces a variety of species: unphotolyzed, singly photolyzed, doubly photolyzed, singly inactivated, doubly inactivated, and singly photolyzed-singly inactivated, with a variety of transition probabilities among species (Fryer and Zucker, 1993). Unphotolyzed diazo-4 is highly absorbent (46,000 M^{-1} cm^{-1} at 371 nm for the free form; about 4600 M^{-1} cm^{-1} for the Ca^{2+}-bound form). The singly photolyzed species have absorbances of half these values and doubly photolyzed diazo-4 has negligible absorbance at this wavelength. Inactivation causes little change in absorbance.

A third member of this series, diazo-3, has a diazoketone attached to half the cation-coordinating structure of BAPTA, and has negligible Ca^{2+} affinity. On photolysis, diazo-3 produces the photochemical intermediates of diazo-2 plus a proton, and may be used to control for these effects of photolysis of the diazo series. At one time, diazo-2 and diazo-3 (but not diazo-4) were commercially available (Molecular Probes, Eugene, and Oregon), but these stocks appear to have been exhausted.

B. Calculating Effects of Photolysis

As for the nitr compounds, equilibration is faster than photolysis, so a flash of light leads to a smooth step transition in the concentration of Ca^{2+} chelator species. If the percentage of photolysis caused by a light flash is known, the proportions of photolyzed and inactivated diazo-2, or of the six species of diazo-4, can be calculated. Usually, diazo is injected without any added Ca^{2+}, so the effect of photoreleased buffers is to reduce the $[Ca^{2+}]_i$ from its resting value. This change can be calculated only if the total Ca^{2+} bound to the native buffer in cytoplasm as well as the characteristics of that buffer are known. These characteristics often can be inferred from available measurements on cytoplasmic Ca^{2+} buffer power and the normal resting $[Ca^{2+}]_i$ level. The more usual application of these substances is to reduce the effect of a physiologically imposed rise in $[Ca^{2+}]_i$. In many cases, the magnitude of the source of this Ca^{2+} is known, as in the case of a Ca^{2+} influx measured as a Ca^{2+} current under voltage clamp or the influx through single channels estimated from single channel conductances. Also, the magnitude of the total Ca^{2+} increase in a response can be estimated from measured increases in $[Ca^{2+}]$; and estimates of cytoplasmic buffering. With this information, the expected effect of newly formed diazo photoproducts on a physiological rise in $[Ca^{2+}]_i$ can be calculated by solving diffusion equations that are appropriate for the distribution of Ca^{2+} sources before and after changing the composition of the

mixture of buffers in the cytoplasm. Examples of such solutions of the diffusion equation exist for spherical diffusion inward from the cell surface (Nowycky and Pinter, 1993; Sala and Hernández-Cruz, 1990), cylindrical diffusion inward from membranes of nerve processes (Stockbridge and Moore, 1984; Zucker and Stockbridge, 1983), diffusion from a point source (Fryer and Zucker, 1993; Stern, 1992), and diffusion from arrays of point sources (Fogelson and Zucker, 1985; Matveev *et al.*, 2002, 2004, 2006, 2009; Pan and Zucker, 2009; Simon and Llinás, 1985; Tang *et al.*, 2000; Yamada and Zucker, 1992). For large cells, the spatial nonuniformity of light intensity and photolysis rate also must be considered, taking into account the absorbances of all the species of diazo and the changes in their concentration with photolysis. Like azid-1, the self-screening imposed by diazo chelators is reduced with photolysis, so successive flashes (or prolonged illumination) are progressively more effective.

V. Introduction into Cells

Photolabile chelators are introduced into cells by pressure injection from micropipettes, perfusion from whole-cell patch pipettes, or permeabilization of the cell membrane. Iontophoresis is also suitable for diazo compounds, since this procedure inserts only the Ca^{2+}-free form. For the caged Ca^{2+} substances, this method of introduction requires that the chelator load itself with Ca^{2+} by absorbing it from cytoplasm or intracellular stores. Filling cells from a patch pipette has the special property that, if the photolysis light is confined to the cell and excludes all but the tip of the pipette inside the cell, the pipette barrel acts as an infinite reservoir of unphotolyzed chelator. Then the initial conditions of solutions in the pipette can be restored within minutes after photolysis of the chelator in the cell. The nitr and diazo compounds are soluble at concentrations over 100 mM and DM-nitrophen is soluble at 75 mM, so levels in cytoplasm exceeding 10 mM can be achieved relatively easily, even by microinjection, making the exogenous chelator compound the dominant buffer.

Nitr and diazo chelators also have been produced as membrane-permeant acetoxymethyl (AM) esters (Kao *et al.*, 1989). Exposure of intact cells to medium containing these esters (available from CalBiochem and Molecular Probes, respectively) might result in the loading of cells with nearly millimolar concentrations, if sufficient activity of intracellular esterase is present to liberate the membrane-impermeant chelator. However, nitr-5 or nitr-7 introduced in this manner is not bound to Ca^{2+}, so it must sequester Ca^{2+} from cytoplasm, from intracellular stores, or after Ca^{2+} influx is enhanced, for example, by depolarizing excitable cells. The final concentration, level of Ca^{2+} loading, and localization of the chelator are uncertain, so this method of incorporation does not lend itself to quantification of effects of photolysis unless cells are coloaded with a Ca^{2+} indicator.

During loading and other preparatory procedures, the photolabile chelators may be protected from photolysis with low pass UV-blocking filters in the light path of the

tungsten or quartz halide beams used for viewing. For more detail on these filling procedures, see Gurney (1991). Other methods of loading cells, used primarily with other sorts of caged compounds, are discussed by Adams and Tsien (1993).

VI. Light Sources

Photolysis of caged Ca^{2+} chelators requires a bright source of near UV light. If speed is unimportant, an ordinary mercury or xenon arc lamp may be used. Mercury lamps have a convenient emission line at 366 nm. Exposure can be controlled with a shutter, using MgF-coated Teflon blades for particularly bright sources. Lamps of 100–150 W power with collimating quartz lenses provide sufficient energy to photolyze ~25% of caged Ca^{2+} compounds in ~2 s. Bulbs of larger power only generate bigger arcs, with more energy in a larger spot of similar intensity. With additional focusing, photolysis can be achieved in one-tenth the time or even less. These light sources are the appropriate choice in applications using reversible $[Ca^{2+}]_i$ elevation with DM-nitrophen.

Fast events require the use of a laser or xenon arc flashlamp. The xenon lamps are less expensive and cumbersome; convenient commercial systems are available from Chadwick-Helmuth (El Monte, California), Rapp Optoelektronik (Hamburg, Germany), TILL Photonics (Gräfelting, Germany), and Cairn Research (Faversham, UK). These flashlamps discharge up to 200–300 J electrical energy across the bulb to provide a pulse of ~1 ms duration with up to 300 mJ energy in the 330−380-nm band. The Chadwick-Helmuth unit includes only a power supply and lamp socket, so a housing with focusing optics must be constructed (see Rapp and Guth, 1988). Focusing can be accomplished with a UV-optimized elliptical reflector or with quartz refractive optics. The reflector can be designed to capture more light (i.e., have a larger effective numerical aperture), but reflectors have greater physical distortion than well-made lenses. In practice, the reflector generates a larger spot with more total energy, but somewhat less intensity, than refractive methods. One advantage of reflectors is that they are not subject to chromatic aberration—focusing is independent of wavelength—so the UV will be focused in the same spot as visual light. This is not true of refractive lenses. To focus and aim them accurately at the sample, a UV filter must be used to block visual light and the beam must be focused on a fluorescent surface for visualization. Both types of housing are available from Rapp Optoelektronik. Using either system, photolysis rates approaching 80–90% in one flash are achievable. This rate may be reduced by imposing neutral density filters or reducing discharge energy, but the relationship between electrical and light energy is not linear and should be measured with a photometer. Flashlamps can be reactivated only after their storage capacitors have recharged, setting the minimal interval between successive maximal flashes at several seconds or more.

F1ashlamps are prone to generating a number of artifacts. The discharge causes electrical artifacts that can burn out semiconductors and op amps, and reset or

clear digital memory in other nearby equipment. Careful electrostatic shielding, wrapping inductors with paramagnetic metal, power source isolation, and using isolation circuits in trigger pulse connections to other equipment prevent most problems, which are also diminished in pulsed mercury lamps (Denk, 1997). The discharge generates a mechanical thump at the coil used to shape the current pulse through the bulb; this thump can dislodge electrodes from cells or otherwise damage the sample. Mechanical isolation of the offending coil solves the problem. Lamp discharge also produces an air pressure pulse that can cause movement artifacts at electrodes, which can be seen to oscillate violently for a fraction of a second when videotaped during a flash. This movement can damage cells severely, especially those impaled with multiple electrodes. Small cells sealed to the end of a patch pipette often fare better against such mistreatment. To reduce this source of injury, the light can be filtered to eliminate all but the near UV. Commercial Schott filters (UG-I, UG-Il), coated to reflect infrared (IR) light, serve well for this purpose, but can cut the 330–380-nm energy to 30% or less. Liquid filters to remove IR and far UV also have been described (Tsien and Zucker, 1986). Removing IR reduces temperature changes, which otherwise can exceed 1 °C per flash, whereas removing far UV prevents the damaging effects of ionizing radiation. Chlorided silver pellets and wires often used in electrophysiological recording constitute a final source of artifact. These components must be shielded from the light source or they will generate large photochemical signals.

To simply aim and focus the light beam directly onto the preparation is easiest. If isolating the lamp from the preparation is necessary, the light beam may be transmitted by a fiber optic or liquid light guide, with some loss of intensity. If a microscope is being used already, the photolysis beam may be directed through the epifluorescence port of the microscope. The lamp itself, or a light guide, may be mounted onto this port. Microscope objectives having high numerical aperture and good UV transmission will focus the light quite effectively onto a small area, which can be delimited further by a field stop aperture. With the right choice of objectives and proper optical coupling of the lamp to the light guide and the guide to the microscope port, light intensities 25 times greater than those obtained by simply aiming the focused steady lamp or flashlamp can be achieved—sufficient to half-photolyze DM-nitrophen in 25 ms of steady bright light. TILL Photonics make a xenon arc spectrophotometer (the Polychrome) with efficient optical coupling to several commercial epifluorescence microscopes. Half reflective mirrors can be used to combine the photolysis beam with other light sources, such as those used for $[Ca^{2+}]_i$ measurement. However, as the optical arrangement becomes more complex, photolysis intensity inevitably decreases.

The newest development in light sources is the high intensity light-emitting diode (Bernardinelli *et al.*, 2005). This rapidly evolving and inexpensive technology can already produce 365-nm UV light at 50 mW/cm^2 (with LEDs made by Prizmatix, Modi'in Ilite, Israel, e.g.), or about 20% of the intensity of a collimated xenon arc lamp.

It is often important to restrict photolysis to one region of a cell (Wang and Augustine, 1995). With epi-illumination, this may be done with a field stop

diaphragm, or by conveying the photolysis beam through a tapered quarty fiber optic filter to the cell surface (Eberius and Schild, 2001; Godwin *et al.*, 1997). Lasers provide an alternative source of light with the advantages of a coherent collimated beam that is focused much more easily to a very small spot. Pulsed lasers such as the frequency-doubled ruby laser or the XeF excimer laser provide at least 200 mJ energy at 347 or 351 nm in 50 and 10 ns, with possible repetition rates of 1 and 80 Hz, respectively. Liquid coumarin-dye lasers, with up to 100 mJ tunable energy in the UV and pulse duration, are also available. Inexpensive nitrogen lasers providing lower pulse energies (0.25 mJ) in 5-ns pulses at 337 nm also have been developed (Engert *et al.*, 1996) and, with appropriate focusing, might be useful. To date, lasers have found their widest application in studies of muscle contraction. More information on these laser options is contained in discussions by Goldman *et al.* (1984) and McCray and Trentham (1989).

An adaptation of laser photolysis is the two-photon absorption technique (Denk *et al.*, 1990). A colliding-pulse mode-locked Ti:Sapphire laser generating 100-fs pulses of 630-nm light at 80 MHz is focused through a confocal scanning microscope. Photolysis of UV-sensitive caged compounds requires simultaneous absorption of two red photons, so photolysis occurs only in the focal plane of the scanning beam. This behavior restricts photolysis to about 1 μm^3 in three dimensions, but for most compounds the photolysis rate is so slow, due to their extremely limited two-photon cross sections, that several minutes of exposure are required with currently available equipment. The best results were achieved with azid-1 and NDBF-EGTA (Brown *et al.*, 1999; DelPrincipe *et al.*, 1999; Momotake *et al.*, 2006), as expected from their high single photon absorbances. Azid-1 could be fully photolyzed in the two-photon focal volume with a 10-μs pulse train of 7 mW average power, with a retention time of the released Ca^{2+} in this volume of about 150 μs. This technique is expensive and specialized, and is still under development, but may have practical applications in revealing the precise localization within cells or subcellular organelles of fixed targets of Ca^{2+} action or of highly localized Ca^{2+} buffers.

Near-UV light alone seems to have little effect on most biological tissues, with the obvious exception of photoreceptors and the less obvious case of smooth muscle (Gurney *et al.*, 1987). Control experiments on the effects of light on unloaded cells, and on the normal physiological response under study, can be used to ascertain the absence of photic effects.

VII. Calibration

When designing a new optical system or trying a new caged compound, being able to estimate the rate of photolysis of the apparatus used is important. This information is necessary to adjust the light intensity or duration for the desired degree of photolysis, and to insure that photolysis is occurring at all.

In principle, the fraction (F) of a substance photolyzed by a light exposure of energy J can be computed from the formula $e^{-(J-J')} = (I-F)/0.1$, where J' is the

energy needed to photolyze 90% of the substance and is given by $J' = hcA/Q\varepsilon\lambda$, where h is Planck's constant, c is the speed of light, A is Avogadro's number, Q is the quantum efficiency, ε is the decadic molar extinction coefficient, and λ is the wavelength of the light. In practice, however, this equation is rarely useful for the following reasons.

1. Measuring the energy of the incident light on a cell accurately is difficult, especially for light of broad bandwidth with varying intensity at different wavelengths.

2. The quantum efficiency, although provided for all the photolabile chelators, is not such a well-defined quantity. The value depends critically on how it is measured, which is not always reported. In particular, the effective quantum efficiency for a pulse of light of moderate duration (e.g., from a flashlamp) is often greater than that of either weak steady illumination or a very brief pulse (e.g., from a laser), because of the possibility of multiple photon absorptions of higher efficiency by photochemical intermediates. This phenomenon has been noted to play a particularly strong role in nitr-5 photolysis (McCray and Trentham, 1989). Thus, apparent differences in quantum efficiencies between different classes of chelators may be mainly the results of different measurement procedures.

3. Finally, the quantum efficiency is a function of wavelength, which is rarely given.

A more practical and commonly adopted approach is mixing a partially Ca^{2+}-loaded photolabile chelator with a Ca^{2+} indicator in a solution with appropriate ionic strength and pH buffering, and measuring the $[Ca^{2+}]$ change in a small volume of this solution, the net absorbance of which is sufficiently small to minimize inner filtering of the photolyzing radiation. Suitable indicators include fura-2, indo-1 (Grynkiewicz *et al.*, 1985), furaptra (Konishi *et al.*, 1991), f1uo-3, rhod-2 (Minta and Tsien, 1989), Calcium Green™, Orange™, and Crimson™ (Eberhard and Erne, 1991), arsenazo III (Scarpa *et al.*, 1978), and fura-red (Kurebayashi *et al.*, 1993). The choice depends largely on available equipment. Fura-2, indo-1, and furaptra are dual-excitation or-emission wavelength fluorescent dyes, allowing more accurate ratiometric measurement of $[Ca^{2+}]$, but they require excitation at wavelengths that photolyze the photolabile Ca^{2+} chelators and are subject to bleaching by the photolysis light. The former problem may be minimized by using low intensity measuring light with a high sensitivity detection system. Furaptra is especially useful for DM-nitrophen, because of its lower Ca^{2+} affinity. Fluo-3 and rhod-2 were designed specifically for use with photolabile chelators (Kao *et al.*, 1989), being excited at wavelengths different from those used to photolyze the chelators, but they are not ratiometric dyes and are difficult to calibrate accurately. Calcium Green, Orange, and Crimson suffer the same limitation, but they are often used because of their fast kinetics and bright intensity, allowing the accurate tracking of fast changes in $[Ca^{2+}]_i$. Arsenazo and antipyralazo are metallochromic dyes that change absorbance on binding Ca^{2+},

fortunately at wavelengths different from those at which the photolabile chelators show any significant absorbance. However, these dyes are also difficult to calibrate for absolute levels of $[Ca^{2+}]$, although changes in $[Ca^{2+}]$ may be determined fairly accurately. Fura-red is a ratiometric dye excited by visible light, so it might have some application in calibrating photolysis. A problem common to all the fluorescent indicators is that their fluorescent properties may be altered by the presence of photolabile chelators, which generally are used at millimolar levels whereas the indicators are present at 100 μM or less. The photolabile chelators often produce contaminating fluorescence, which also may be Ca^{2+}-dependent and may partially quench the fluorescence of the indicators (Hadley *et al.*, 1993; Zucker, 1992). Thus, the indicators must be calibrated in the presence of photolabile chelator at three well-controlled $[Ca^{2+}]$ levels, preferably before and after exposure to the photolysis flash, before they can be used to measure the effects of photolysis on $[Ca^{2+}]$ (Neher and Zucker, 1993). The low and high $[Ca^{2+}]$ calibrating solutions may be made with excess Ca^{2+} or another buffer such as EGTA or BAPTA, but the intermediate $[Ca^{2+}]$ solution is more difficult to generate, since photolysis of the chelator will release some Ca^{2+} and change the $[Ca^{2+}]_i$ and pH in this solution unless it contains a very high concentration of controlling chelator and pH buffer.

The calibration procedure is generally the same for any combination of chelator and indicator. A small sample of the mixture is placed in a 1-mm length of microcuvette with a 20-μm pathlength (Vitro Dynamics, Rockaway, New Jersey) under mineral oil to prevent evaporation. This cuvette is exposed repeatedly to the photolysis beam or to flashes, which should illuminate the whole cuvette uniformly, and the $[Ca^{2+}]$ after each flash or exposure is measured using a microscope-based fluorescence or absorbance photometer. A small droplet of solution under mineral oil alone would work, and may be necessary if the photolysis beam is directed through the microscope and illuminates a very small area, but sometimes the fluorescent properties of the indicators are affected by the mineral oil. This effect would be detected in the procedure for calibrating the chelator-indicator mixture, but is best avoided using the microcuvettes, in which contact with oil is only at the edges, the fluorescence or absorbance change of which need not be measured. In some applications, such as whole-cell patch clamping of cultured cells, using the cell as a calibration chamber can be easier than any other procedure.

The expected changes in $[Ca^{2+}]$ depend on the chelator used. The nitr and diazo chelators should lead to a stepwise rise or fall in $[Ca^{2+}]$ after each exposure; the results can be fitted to models of the chelators and their photoproducts, using their affinities and the relative quantum efficiencies of free and bound chelators (Fryer and Zucker, 1993; Landò and Zucker, 1989). The percentage photolysis of the chelator in response to each light exposure is the only free parameter, and is varied until the model fits the results. In the case of the high-affinity DM-nitrophen, little rise in $[Ca^{2+}]$ will occur until the total amount of remaining unphotolyzed chelator equals the total amount of Ca^{2+} in the solution, whereupon the $[Ca^{2+}]$ will increase suddenly. Equations relating initial and final concentrations of DM-nitrophen,

total [Ca^{2+}], and photolysis rate (Zucker, 1993) then may be used to calculate photolysis rate per flash or per second of steady light exposure.

Most photosensitive compounds also undergo substantial absorbance changes after photolysis. These changes can be monitored during repeated exposure to the light source without a Ca^{2+} indicator; the number of flashes or the duration of light exposure required to reach a given percentage photolysis then can be determined. Realizing that photolysis proceeds exponentially to completion (Zucker, 1993), these data can be used to determine the photolysis rate directly. Ideally, both methods should be used to check for consistent results. A final method for determining photolysis rate is using high pressure liquid chromatography (HPLC) to separate and quantify parent chelators and photoproducts in the reaction solution after partial photolysis (Walker, 1991).

VIII. Purity and Toxicity

When experiments do not work as planned, the first suspected source of error is the integrity of the photolabile chelator. Different procedures have proved most useful for testing the different classes of compounds. The nitr and diazo compounds undergo large absorbance changes on binding calcium and photolysis. A 100 μM solution (nominally) of the chelator is mixed with 50 μM Ca^{2+} in 100 mM chelexed HEPES solution (pH 7.2), and 0.3 ml is scanned in a 1-mm pathlength spectrometer. Then 1 μl 1 M K_2EGTA is added to bring the [Ca^{2+}] to 0, and the sample is scanned again. Finally, 1 μl 5 M $CaCl_2$ is added to provide excess Ca^{2+}, and a third scan is recorded. The first scan should be midway between the other two. If the first scan is closer to the excess Ca^{2+} scan, it is indicative of a lower than expected concentration of the chelator, probably because of an impurity. Alternatively, Ca^{2+} may have been present with the chelator, which may be checked by running a scan on the chelator with no added Ca^{2+} and comparing the result with a scan with added EGTA; they should be identical. Ca^{2+} free and Ca^{2+}-saturated chelator solutions also are scanned before and after exposure to UV light sufficient to cause complete photolysis; the spectra are compared with published figures (Adams *et al.*, 1988, 1989; Kaplan and Ellis-Davies, 1988) to determine whether the sample was partially photolyzed at the outset. The Ca^{2+} affinities of unphotolyzed and photolyzed chelators can be checked by measuring the [Ca^{2+}] of 50%-loaded chelators with a Ca^{2+}-selective electrode.

The absorbance of DM-nitrophen and some related chelators is almost Ca^{2+} independent, so these procedures are not effective. A solution of DM-nitrophen nominally of 2 mM concentration is titrated with concentrated $CaCl_2$ until the [Ca^{2+}] measured with an ion-selective electrode suddenly increases; this change indicates the actual concentration of the chelator and gives an estimate of purity. The affinity of the photolysis products can be measured as for the other chelators; spectra before and after photolysis indicate whether the sample was already partially photolyzed.

Purities of 80–90% are typical for commercial samples of all the chelators, but occasional batches of 60% purity or less have been seen; these also sometimes show high degrees of toxicity. Whether such low purity is the result of poor synthesis or storage is unclear. Nitr compounds decompose detectably after only 1 day at room temperature, and exposure to ambient fluorescent lighting for 1 day causes detectable photolysis. Chelators should be shipped on dry ice and stored at $-80\,^{\circ}C$ in the dark; even under these conditions they do not last forever. Repeated thawing and freezing also degrades the compounds.

Some of the photolabile Ca^{2+} chelators display a degree of biological toxicity in some preparations. Commercial samples of nitr-5 have been seen to lyse sea urchin eggs (R. S. Zucker and L. F. Jaffe, unpublished results) and leech blastomeres (K. R. Delaney and B. Nelson, unpublished results) within minutes. Zucker and Haydon (1988) found that nitr-5 blocked transmitter release within 10 min of perfusion in snail neurons, whereas DM-nitrophen has no similar effect (P. Haydon, unpublished results). These effects are not caused by the photoproducts, since photolysis is not necessary for the problems to occur. DM-nitrophen has been observed to reduce secretion in chromaffin cells; higher chelator concentrations, photolyzed to give the same final $[Ca^{2+}]_i$ level, caused less secretion (C. Heinemann and E. Neher, unpublished results). The effect was overcome partially by inclusion of glutathione in the perfusion solution, as reported for the photoproducts of other 2-nitrobenzhydrol-based caged compounds (Kaplan *et al.*, 1978). These signs of toxicity have been observed sporadically; whether they are properties of the chelators themselves or of impurities in the samples used is unclear. The chelators have been applied successfully to a wide range of preparations without obvious deleterious results, although subtle effects may have been missed.

IX. Biological Applications

A brief synopsis of the earliest biological applications of the caged Ca^{2+} chelators follows along with a much more selective sampling of the more recent and extensive literature. This is included in this chapter because many of the original papers include a wealth of detail about methodology and interpretation of Ca^{2+} photorelease technology.

A. Ion Channel Modulation

1. Potassium and Nonspecific Cation Channels

The first and still one of the major applications of photosensitive Ca^{2+} chelators is analysis of Ca^{2+}-dependent ion channels in excitable cells. In 1987, Gurney *et al.* first used nitr-2,-5, and-7 to activate Ca^{2+}-dependent K^+ current in rat sympathetic neurons. These researchers found that a single Ca^{2+} ion binds to the channel with rapid kinetics and 350 nM affinity.

The next application of the nitr chelators was in an analysis of Ca^{2+}-activated currents in *Aplysia* neurons (Landò and Zucker, 1989). We found that Ca^{2+}-activated K^+ and nonspecific cation currents in bursting neurons were linearly dependent on $[Ca^{2+}]_i$ jumps in the micromolar range, as measured by arsenazo spectrophotometry and modeling studies. Both currents relaxed at similar rates after photolysis of nitr-5 or nitr-7, reflecting diffusional equilibration of $[Ca^{2+}]_i$ near the front membrane surface facing the light source. Potassium current relaxed more quickly than nonspecific cation current, after activation by Ca^{2+} entry during a depolarizing pulse, because of the additional voltage sensitivity of the K^+ channels. This difference was responsible for the more rapid decay of hyperpolarizing afterpotentials than of depolarizing afterpotentials.

The role of Ca^{2+}-activated K^+ current in shaping plateau potentials in gastric smooth muscle was explored by Carl *et al.* (1990). In fibers loaded with nitr-5/AM, Ca^{2+} photorelease accelerated repolarization during plateau potentials and delayed the time to subsequent plateau potentials, suggesting a role for changes in $[Ca^{2+}]_i$ and Ca^{2+}-activated K^+ current in slow wave generation.

Another current modulated by $[Ca^{2+}]_i$ is the so-called M current, a muscarine-blocked K^+ current in frog sympathetic neurons. Although inhibition is mediated by G-protein coupling of the receptor to phospholipase C, resting M current is enhanced by modest elevation of $[Ca^{2+}]_i$ (some tens of nanomolar) and reduced by greater elevation of $[Ca^{2+}]_i$, which also suppresses the response to muscarine (Marrion *et al.*, 1991). As for ventricular I_{Ca} (see below), several sites of modulation of M current by $[Ca^{2+}]_i$ apparently exist. In these experiments, $[Ca^{2+}]_i$ was elevated by photorelease from nitr-5 and simultaneously measured with fura-2. Step changes in $[Ca^{2+}]_i$ imposed by diazo-2 photolysis and monitored with bis-fura-2 fluorescence changes have also been used to characterize the modulation of cGMP-gated ion channels by $[Ca^{2+}]_i$ (Rebrik *et al.*, 2000).

The after-hyperpolarization that follows spikes in rat hippocampal pyramidal neurons is caused by a class of Ca^{2+}-dependent K^+ channels called I_{AHP} channels. This after-hyperpolarization and the current underlying it rise slowly to a peak 0.5 s after the end of a brief burst of spikes. Ca^{2+} photorelease from nitr-5 or DM-nitrophen activates this current without delay (Lancaster and Zucker, 1994), and the current may be terminated rapidly by photolysis of diazo-4 (but see conflicting results of Sah and Clements, 1999), suggesting that the delay in its activation following action potentials is caused by a diffusion delay between points of Ca^{2+} entry and the I_{AHP} channels.

The Ca^{2+} sensitivity of the mechanoelectrical transduction current in chick cochlear hair cells was studied using nitr-5 introduced by hydrolysis of the AM form (Kimitsuki and Ohmori, 1992). Elevation of $[Ca^{2+}]_i$ to 0.5 μM (measured with fluo-3) diminished responses to displacement of the hair bundle, and accelerated adaptation during displacement when Ca^{2+} entry occurred. Preventing Ca^{2+} influx blocked adaptation. Evidently, adaptation of this current was the result of an action of Ca^{2+} ions entering through the transduction channels.

In guinea pig hepatocytes, noradrenaline evokes a rise in K^+ conductance after a seconds-long delay. Photorelease of Ca^{2+} from nitr-5 and use of caged inositol

1,4,5-trisphosphate (caged-IP_3) show that this delay arises from steps prior to or during generation of IP_3 (Ogden *et al.*, 1990), which releases Ca^{2+} from intracellular stores to activate K^+ current.

2. Calcium Channels

The first application of DM-nitrophen was in a study of Ca^{2+} channels in chick dorsal root ganglion neurons (Morad *et al.*, 1988). With divalent charge carriers, inactivation by photorelease of intracellular Ca^{2+} occurred within 7 ms, whereas with monovalent charge carriers a nearly instantaneous block occurred, especially when Ca^{2+} was released extracellularly. A similar rapid block of monovalent current through Ca^{2+} channels was observed in response to photorelease of extracellular Ca^{2+} in frog ventricular cells (Näbauer *et al.*, 1989). Different Ca^{2+}-binding sites may be exposed if altered conformational states are induced in the channels by the presence of different permeant ions.

The regulation of Ca^{2+} current (I_{Ca}) in frog atrial cells by $[Ca^{2+}]_i$ also has been studied with nitr-5 (Charnet *et al.*, 1991; Gurney *et al.*, 1989). Rapid elevation of $[Ca^{2+}]_i$ potentiated high-voltage-activated or L-type I_{Ca} and slowed its deactivation rate when Ba^{2+} was the charge carrier, after a delay of several seconds. Inclusion of BAPTA in the patch pipette solution blocked the effect of nitr-5 photolysis. The similarity of effect of Ca^{2+} and cAMP and their mutual occlusion suggest a common phosphorylation mechanism.

Regulation of I_{Ca} in guinea pig ventricular cells appears to be more complex (Bates and Gurney, 1993; Hadley and Lederer, 1991). A fast phase of inactivation reflects a direct action on Ca^{2+} channel permeation, since I_{Ca} inactivation caused by photorelease of Ca^{2+} from nitr-5 is independent of the phosphorylation state of the channels and does not alter gating currents. A late potentiation is also present, the magnitude of which depends on the flash intensity delivered during a depolarizing pulse, but not on the initial $[Ca^{2+}]_i$ level, the degree of loading of nitr-5, or the presence of BAPTA in the patch pipette. This result suggests that, during a depolarization, nitr-5 becomes locally loaded by Ca^{2+} entering through Ca^{2+} channels, and that the Ca^{2+}-binding site regulating potentiation is near the channel mouth. Larger $[Ca^{2+}]_i$ jumps elicited by photolysis of DM-nitrophen evoke greater I_{Ca} inactivation, but no potentiation, perhaps because of the more transient rise in $[Ca^{2+}]_i$ when DM-nitrophen is photolyzed.

DM-nitrophen loaded with magnesium in the absence of Ca^{2+} was used to study the Mg^{2+}-nucleotide regulation of L-type I_{Ca} in guinea pig cardiac cells (Backx *et al.*, 1991; O'Rourke *et al.*, 1992). In the presence of ATP, a rise in $[Mg^{2+}]_i$ to 50–200 μM led to a near doubling of the magnitude of I_{Ca}. Release of caged ATP also increased I_{Ca}. Therefore, the effect on Ca^{2+} channels was caused by a rise in Mg^{2+}-ATP. Nonhydrolyzable ATP analogs worked as well as ATP, so Mg^{2+}-ATP seems to modulate Ca^{2+} channels directly.

We microinjected *Aplysia* neurons with nitr-5, DM-nitrophen, or diazo-4 to characterize Ca^{2+}-dependent inactivation of Ca^{2+} current (Fryer and Zucker,

1993). Elevation of $[Ca^{2+}]_i$ to a few micromolar with nitr-5 caused little inactivation, but photolysis of DM-nitrophen rapidly inactivated half the I_{Ca}, presumably that in the half of the cell facing the light source. Thus, inactivation requires high $[Ca^{2+}]_i$ levels and occurs rapidly in all channels, even if they are closed. Experiments with diazo-4 showed that an increase in buffering power reduced the rate of inactivation of I_{Ca} modestly. Diffusion-buffer reaction simulations suggest that Ca^{2+} acts at a site within 25 nm of the channel mouth (see also Johnson and Byerly, 1993).

B. Muscle Contraction

One of the earliest applications of photolabile Ca^{2+} chelators was initiating muscle contraction in frog cardiac ventricular cells by photorelease of extracellular Ca^{2+} from DM-nitrophen (Näbauer *et al.*, 1989). The strength of contraction elicited by a stepwise rise in $[Ca^{2+}]_e$ showed a membrane potential dependence that was indicative of entry through voltage-dependent Ca^{2+} channels rather than of transport by Na^+–Ca^{2+} exchange.

Several laboratories have used caged Ca^{2+} chelators to study Ca^{2+}dependent Ca^{2+} release from the sarcoplasmic reticulum in rat ventricular myocytes. Valdeolmillos *et al.* (1989) loaded cells with the AM form of nitr-5, Kentish *et al.* (1990) subjected saponin-skinned fibers to solutions containing Ca^{2+}-loaded nitr-5, and Näbauer and Morad (1990) perfused single myocytes with DM-nitrophen loaded with Ca^{2+}. Photolysis elicited a contraction blocked by ryanodine or caffeine, procedures that prevent release of Ca^{2+} from the sarcoplasmic reticulum, implicating Ca^{2+}-induced Ca^{2+} release, which could be confined to a portion of a fiber by localized photolysis (O'Neill *et al.*, 1990).

Györke and Fill (1993) used Ca^{2+}-DM-nitrophen to show that the cardiac ryanodine receptors adapt to maintained $[Ca^{2+}]_i$ elevation, remaining sensitive to larger $[Ca^{2+}]_i$ changes and responding by releasing still more Ca^{2+}. In smooth muscle from guinea pig portal vein, the IP_3-dependent release of Ca^{2+} was itself dependent upon $[Ca^{2+}]_i$ (Iino and Endo, 1992). Ca^{2+} photoreleased from DM-nitrophen and measured with fluo-3 accelerated Ca^{2+} release from a ryanodine-insensitive, IP_3-activated store. The possibility that adaptation reflected slow unbinding of Ca^{2+} from the channels following a flash-induced Ca^{2+} "spike" was refuted by demonstrating a rapid deactivation of channel function to a sudden drop in $[Ca^{2+}]_i$ imposed by diazo-2 (Vélez *et al.*, 1997).

Ca^{2+}-loaded nitr-5 was used in skinned frog and scallop muscle fibers to show that the rate-limiting step in contraction is not the time-course of the rise in $[Ca^{2+}]_i$ but rather the response time of the contractile machinery (Ashley *et al.*, 1991b; Lea and Ashley, 1990). Using isolated myofibrillar bundles from barnacle muscle, Lea and Ashley (1990) showed that nitr-5 photolysis elevating $[Ca^{2+}]_i$ by 0.2–1.0 μM Ca^{2+} not only activated contraction directly and rapidly but also evoked a slower phase of contraction that was dependent on Ca^{2+}-induced Ca^{2+} release from the sarcoplasmic reticulum. Analysis of $[Ca^{2+}]_i$ steps imposed by DM-nitrophen or

diazo-2 revealed kinetics of muscle contraction and relaxation steps following the binding and unbinding of Ca^{2+} to troponin C (Ashley *et al.*, 1993).

The first biological application of the caged chelator diazo-2 was in the study of muscle relaxation. Mulligan and Ashley (1989) showed that rapid reduction in $[Ca^{2+}]_i$ in skinned frog semitendinosus muscle resulted in a relaxation similar to that occurring normally in intact muscle, indicating that mechanochemical events subsequent to the fall in $[Ca^{2+}]$ were rate limiting. However, Lannergren and Arner (1992) reported some speeding of isometric relaxation after photolysis of diazo-2, loaded in the AM form into frog lumbrical fibers. Lowered pH slowed relaxation to a step reduction in $[Ca^{2+}]_i$ (Palmer *et al.*, 1991), perhaps accounting for a contribution of low pH to the sluggish relaxation of fatigued muscle. In contrast to frog muscle, photorelease of Ca^{2+} chelator caused a much faster relaxation in skinned scallop muscle than in intact fibers (Palmer *et al.*, 1990), suggesting that, in these cells, relaxation is rate limited primarily by $[Ca^{2+}]_i$ homeostatic processes.

C. Synaptic Function

Action potentials evoke transmitter release in neurons by admitting Ca^{2+} through Ca^{2+} channels. Because of the usual coupling between depolarization and Ca^{2+} entry, assessing the possibility of an additional direct action of membrane potential on the secretory apparatus has been difficult. Photolytic release of presynaptic Ca^{2+} by nitr-5 perfused into presynaptic snail neurons cultured in Ca^{2+}-free media was combined with voltage clamp of the presynaptic membrane potential to distinguish the roles of $[Ca^{2+}]_i$ and potential in neurosecretion (Zucker and Haydon, 1988), revealing no direct effect of membrane potential on transmitter release.

Hochner *et al.* (1989) injected Ca^{2+}-loaded nitr-5 into crayfish motor neuron preterminal axons, and used a low-$[Ca^{2+}]$ medium to block normal synaptic transmission. They found that action potentials transiently accelerated transmitter release evoked by modest photolysis of nitr-5. However, Mulkey and Zucker (1991) used fura-2 to show that the extracellular solutions used by Hochner *et al.* (1989) failed to block Ca^{2+} influx through voltage-dependent Ca^{2+} channels. When external Ca^{2+} chelators or channel blockers eliminated influx completely, spikes failed to have any influence on transmitter release, even when it was activated strongly by photolysis of intracellularly injected Ca^{2+}-loaded DM-nitrophen.

Delaney and Zucker (1990) confirmed at the squid giant synapse that in a Ca^{2+}-free medium, action potentials have no effect on transmitter release triggered by a rise in $[Ca^{2+}]_i$ upon photolysis of presynaptically injected DM-nitrophen. Flash photolysis of DM-nitrophen produced a transient postsynaptic response resembling normal excitatory postsynaptic potentials. The intense phase of transmitter release was probably caused by the brief spike in $[Ca^{2+}]_i$ following partial photolysis of partially Ca^{2+}-loaded DM-nitrophen. This response began a fraction of a millisecond after the rise in $[Ca^{2+}]_i$, a delay similar to the usual synaptic delay

following Ca^{2+} influx during an action potential; both delays had the same temperature dependence. Thus photolysis of DM-nitrophen caused a $[Ca^{2+}]_i$ transient resembling that occurring normally at transmitter release sites in the vicinity of Ca^{2+} channels that open briefly during an action potential. After the secretory burst, a moderate phase of transmitter release persisted for 15 ms, corresponding to a relaxation in $[Ca^{2+}]_i$ measured with fura-2 that probably reflected slow Ca^{2+} displacement of Mg^{2+} bound to unphotolyzed DM-nitrophen.

Similar responses to partial flash photolysis of lightly Ca^{2+}-loaded DM-nitrophen were observed at crayfish neuromuscular junctions (Landò and Zucker, 1994). Transmitter release evoked by slow photolysis of Ca^{2+}-DM-nitrophen using steady illumination also has been studied at this junction (Mulkey and Zucker, 1993). The rate of quantal transmitter release, measured as the frequency of miniature excitatory junctional potentials (MEJPs), was increased $\sim$1000-fold during the illumination. Brief illumination (0.3–2 s) evoked a rise in MEJP frequency that dropped abruptly back to normal when the light was extinguished, as would be expected from the reversible rise in $[Ca^{2+}]_i$ that should be evoked by such illumination, which leaves most of the DM-nitrophen unphotolyzed (Zucker, 1993). Longer light exposures caused an increase in MEJP frequency that outlasted the light signal, as would be expected from the rise in resting $[Ca^{2+}]_i$ after photolysis of most DM-nitrophen. These experiments illustrate the utility of steady photolysis of partially Ca^{2+}-loaded DM-nitrophen in generating reversible changes in $[Ca^{2+}]_i$ in cells.

At cultured snail synapses, FMRFamide inhibits asynchronous transmitter release elicited by $[Ca^{2+}]_i$ elevated by photolysis of presynaptic nitr-5 (Man-Son-Hing *et al.*, 1989), and blocks synchronous release to partial flash photolysis of partially Ca^{2+}-loaded DM-nitrophen (Haydon *et al.*, 1991). As at crayfish and squid synapses, these flash-evoked postsynaptic responses resembled the spike-evoked responses and were triggered by the spike in $[Ca^{2+}]_i$ that results when DM-nitrophen is used in this fashion.

At leech serotonergic synapses, a presynaptic Ca^{2+} uptake process may be activated by photolysis of presynaptic DM-nitrophen; blocking it with zimelidine or by external Na^+ removal eliminated the presynaptic transport current and prolonged the postsynaptic response, uncovering a contribution of this process to the termination of transmitter release (Bruns *et al.*, 1993).

DM-nitrophen has been used extensively to probe the steps involved in exocytosis in endocrine cells. Measuring $[Ca^{2+}]_i$ changes with furaptra, we and others (Heinemann *et al.*, 1994; Neher and Zucker, 1993; Thomas *et al.*, 1993) observed—in bovine chromaffin cells and rat melanotrophs—three kinetic secretory phases in response to $[Ca^{2+}]_i$ steps to $\sim$100 μM, reflecting release from different vesicle pools. Prior exposure to a modest $[Ca^{2+}]_i$ rise primed phasic responses to a subsequent step in $[Ca^{2+}]_i$, indicating that $[Ca^{2+}]_i$ not only triggers exocytosis but also mobilizes vesicles into a docked or releasable status. After exocytosis, another $[Ca^{2+}]_i$ stimulus often evoked a rapid reduction in membrane capacitance signaling a $[Ca^{2+}]_i$-dependent compensatory endocytosis.

The release of synaptic transmitter by action potentials is often enhanced for about a second after short bouts of presynaptic activity (synaptic facilitation), and for much longer after sustained activity lasting minutes (posttetanic potentiation, PTP). We have used photolytic release of presynaptic Ca^{2+} from DM-nitrophen to induce facilitation without electrical activity (Kamiya and Zucker, 1994). Photolysis of diazo-2 or diazo-4 to terminate the $[Ca^{2+}]_i$ increase lingering briefly after a short spike train abolished facilitation immediately at crayfish neuromuscular junctions. PTP induced by longer stimulation, both in this preparation and in *Aplysia* neuronal synapses (Fischer *et al.*, 1997), was abolished more slowly by rapid reduction of the prolonged residual $[Ca^{2+}]_i$ resulting from mitochondrial overload (Tang and Zucker, 1997). Thus, facilitation and PTP arise from residual $[Ca^{2+}]_i$ acting on distinct molecular targets different from the secretory trigger, which is also activated by Ca^{2+}. We compared responses to $[Ca^{2+}]_i$ steps on flash photolyzing DMNPE-4 at weakly transmitting but strongly facilitating neuromuscular junctions to responses at strongly transmitting but depressible junctions (Millar *et al.*, 2005), and concluded that the difference in response kinetics was best explained by a difference in the state of Ca^{2+}-dependent priming, such that strongly transmitting synapses were already preprimed at rest by a priming target tuned to have a higher Ca^{2+}-sensitivity. This led, in turn, to the development of a comprehensive model of synaptic transmission, facilitation, and depression that comprised three Ca^{2+}-dependent processes—vesicle mobilization to docking sites, priming of docked vesicles, and activation of membrane fusion (Pan and Zucker, 2009).

We (Landò and Zucker, 1989) and Heidelberger *et al.* (1994) were the first to use DM-nitrophen photolysis to characterize the Ca^{2+}-cooperativity of secretion at neuromuscular junctions and retinal bipolar neurons; subsequently, we (Ohnuma *et al.*, 2001) used NP-EGTA and Kasai *et al.* (1999) used DM-nitrophen to show differences in the Ca^{2+}-dependence and sensitivity of peptidergic or aminergic large dense core vesicle fusion and cholinergic small clear vesicle fusion at central molluscan synapses and in PC12 cells. Hsu *et al.* (1996) reported that transmitter release at squid giant synapses decayed to step $[Ca^{2+}]_i$ increases produced by NP-EGTA photolysis; subsequent higher steps evoked more release, indicating transmitter stores had not been depleted, suggesting either an adaptation of the release process, as the authors proposed, or possibly vesicle heterogeneity in sensitivity to release, or the operation of mobilization or priming processes enabling release of previously undocked or unprimed vesicles at higher $[Ca^{2+}]_i$.

Caged Ca^{2+} photolysis has been used extensively in the last decade in many elegant experiments, especially from the laboratories of Erwin Neher and Bert Sakmann, to kinetically characterize in detail the secretory trigger for neurosecretion, primarily at the giant synapse of the calyx of Held (Bollmann and Sakmann, 2005; Bollmann *et al.*, 2000; Felmy *et al.*, 2003a,b; Hosoi *et al.*, 2007; Sakaba *et al.*, 2005; Schneggenburger and Neher, 2000; Wadel *et al.*, 2007; Wang *et al.*, 2004; Young and Neher, 2009). Ca^{2+} uncaging from DM-nitrophen has been used to probe the kinetics and cooperativity of Ca^{2+} binding to the secretory trigger, kinetic consequences of SNARE protein and synaptotagmin mutation, effects of

Ca^{2+} on synaptic facilitation, the dependence of release kinetics on the time-course of local $[Ca^{2+}]_i$ changes, heterogeneity of vesicle Ca^{2+}-sensitivity and release kinetics, the role of Ca^{2+} in mobilizing vesicles to replenished pools depleted in synaptic depression, and to compare secretion evoked by global $[Ca^{2+}]_i$ manipulation in uncaging to local $[Ca^{2+}]_i$ influx though voltage-dependent channels to address the question of distance of the secretory target from Ca^{2+} channels and its changes in development. Kinetic studies of the Ca^{2+}-dependence of secretion using DM-nitrophen have also been conduced on cochlear hair cells (Beutner *et al.*, 2001) and photoreceptors (Duncan *et al.*, 2010).

Zoran *et al.* (1991) used Ca^{2+} photorelease to study synapse maturation. Spike-evoked transmitter release begins only several hours after cultured snail neurons contact a postsynaptic target. DM-nitrophen photolysis showed this developmental change to result from the delayed increase in Ca^{2+}-sensitivity of the secretory machinery.

Long-term potentiation and depression (LTP and LTD) in mammalian cortical synapses are involved in cognitive processes such as memory consolidation and spatial learning. We found that a brief but strong postsynaptic $[Ca^{2+}]_i$ elevation was sufficient to induce LTP in rat hippocampal CA1 synapses onto the injected neuron, while a more prolonged but modest $[Ca^{2+}]_i$ elevation specifically induced LTD, and a brief but modest Ca^{2+} rise could elicit either (Malenka *et al.*, 1988; Neveu and Zucker, 1996a,b; Yang *et al.*, 1999). By terminating the $[Ca^{2+}]_i$ rise following a brief afferent tetanus by photoactivating the Ca^{2+} chelator diazo-4, we showed that postsynaptic $[Ca^{2+}]_i$ must remain elevated for several seconds before it can induce (Malenka *et al.*, 1992). We also found that long-lasting changes in synaptic transmission at CA3 hippocampal pyramidal cells can be produced by postsynaptic $[Ca^{2+}]_i$ elevations induced by DM-nitrophen, NP-EGTA, or DMNPE-4 photolysis (Wang *et al.*, 2004).

A different form of LTD in cerebellar Purkinje neurons that plays a role in motor skill learning, parallel fiber synapses are depressed when their activity coincides with postsynaptic firing, especially when the latter is triggered by climbing fiber input. Lev-Ram *et al.* (1997) showed that photolytic release of caged Ca^{2+} from nitr-7 could replace postsynaptic spiking and that photolytic release of either caged NO or caged cGMP could replace parallel fiber activity; simultaneous uncaging of Ca^{2+} and either NO or cGMP could induce LTD without any electrical stimulation at all. Kasono and Hirano (1994) showed that a modest release of Ca^{2+} from nitr-5 depressed responses to glutamate application to a dendrite only when the stimuli were temporally paired. Using DMNPE-4, Tanaka *et al.* (2007) found that a sufficiently high and prolonged Ca^{2+} elevation alone could induce LTD, and that the threshold for LTD induction was history-dependent.

Depolarization-induced suppression of inhibition (DSI) is another form of cortical synaptic plasticity, which is mediated by activation of postsynaptic endocannabinoid synthesis by activity-induced $[Ca^{2+}]_i$ elevation and subsequent retrograde regulation of inhibitory transmitter release. We found identical DSI

sensitivities to uniform postsynaptic $[Ca^{2+}]_i$ elevation by NP-EGTA photolysis vs. the volume-average of the highly nonuniform $[Ca^{2+}]_i$ elevation on opening voltage-sensitive Ca^{2+} channels by depolarizations (Wang and Zucker, 2001), implying that the enzymatic targets of postsynaptic Ca^{2+} entering through Ca^{2+} channels in activating DSI are not tightly colocalized with the channels—a situation exactly opposite of the case for Ca^{2+} activation of classical transmitter release.

Long-lasting synaptic regulation also occurs at developing neuromuscular junctions, where repeated activation of one of two motor neuron inputs results in a postsynaptic Ca^{2+}-dependent compensatory or homeostatic reduction in presynaptic transmitter release to action potentials at terminals facing the activated receptors. Using focal DM-nitrophen or nitr-5 photolysis to mimic the localized postsynaptic $[Ca^{2+}]_i$ elevation seen to accompany the stimulus normally used to induce this selective persistent depression, we were able to induce a similar synapse-specific modification (Cash *et al.*, 1996a). Subsequently, synapses made by the modified motor neuron onto other muscle fibers also became depressed by the spread of an unidentified presynaptic intracellular signal (Cash *et al.*, 1996b).

D. Other Applications

The tight regulation of cytoplasmic $[Ca^{2+}]_i$ is essential for ensuring that Ca^{2+} can act reliably and efficiently as a localized second messenger of a huge variety of cellular processes. Endogenous buffers play a defining role in this process, and an appreciation of the functions of these buffers and their characteristics (affinities, binding kinetics, mobility, and localization) is crucial to our understanding how Ca^{2+} performs its central cellular functions. Use of photosensitive Ca^{2+} chelators has become an important tool in the estimation of cytoplasmic buffer characteristics, and much effort has gone into developing procedures and protocols for defining them with some precision. Some of the best examples of this sort of analysis come from the laboratories of Stephen Bolsover, Istvan Mody and Julio Vergara, and Erwin Neher, whose papers should be consulted for the analytical details (Faas *et al.*, 2007; Fleet *et al.*, 1998; Nägerl *et al.*, 2000; Naraghi *et al.*, 1998; Xu *et al.*, 1997).

In addition to these major areas of application of caged Ca^{2+} chelators, this method of $[Ca^{2+}]_i$ manipulation has been used to address an increasingly diverse range of biological problems. Nitr and diazo compounds were inserted by AM loading into fibroblasts that were activated by mitogenic stimulation to produce $[Ca^{2+}]_i$ oscillations monitored using f1uo-3 (Harootunian *et al.*, 1988). Photorelease of Ca^{2+} from nitr-5 enhanced and accelerated the oscillations, whereas release of caged chelator by photolysis of diazo-2 inhibited them. Nitr-7 photolysis caused not only an immediate rise in $[Ca^{2+}]_i$ liberated from the photolyzed chelator, but also elicited a later rise in $[Ca^{2+}]_i$ (Harootunian *et al.*, 1991). This effect was shown, pharmacologically, to be caused by IP_3-sensitive stores, suggesting that an interaction between $[Ca^{2+}]_i$ and these stores underlies the $[Ca^{2+}]_i$ oscillations.

Photorelease of Ca^{2+} from DM-nitrophen has been used to study the binding kinetics of Ca^{2+} to the Ca^{2+}-ATPase of sarcoplasmic reticulum vesicles (DeLong

et al., 1990). The relaxation of the [Ca^{2+}] step, measured by arsenazo spectrophotometry after photolysis, revealed the kinetics of binding to the ATPase. Changes in the Fourier transform infrared spectrum consequent to photorelease of Ca^{2+} from nitr-5 provided information on structural changes in the ATPase after binding Ca^{2+} (Buchet *et al.*, 1991, 1992). In a final application to the study of enzyme conformational changes, photolysis of Mg^{2+}-loaded DM-nitrophen was used to form Mg^{2+}-ATP rapidly to activate Na^{+}/K^{+} exchange, the state of which was monitored by fluorescence of aminostyrylpyridinium dyes (Forbush and Klodos, 1991). Rate-limiting steps were measured at 45 s^{-1} by this method.

Ca^{2+} has been implicated in the control of filopodial activity in the responses of growth cones of developing neurons to environmental cues. Pioneer neurons lay out peripheral afferent pathways in developing grasshoppers. We loaded pioneer neurons by de-esterification of the AM esters of DM-nitrophen and calcium green (Lau *et al.*, 1999) and showed that elevation of local $[Ca^{2+}]_i$ in a growth cone to $\sim 1\ \mu M$ for just 10 s was sufficient to activate subsequent filopodial prolongation and induce the formation of new filopodia at spots with high actin concentration (labeled with rhodamine-phalloidin).

In other applications, Gilroy *et al.* (1991) and Fricker *et al.* (1991) microinjected Ca^{2+}-loaded nitr-5 into guard cells of lily leaves and showed that photorelease of about 600 nM intracellular Ca^{2+} (measured with fluo-3) initiated stomatal pore closure. Kao *et al.* (1990) loaded Swiss 3T3 fibroblasts with nitr-5/AM and showed that photolysis that elevated $[Ca^{2+}]_i$ by hundreds of nanomolar (measured by fluo-3) triggered nuclear envelope breakdown, an early step in mitosis, while having little effect on the metaphase to anaphase transition. Control experiments using nitr-9 showed no effect of reactive photochemical intermediates or products. Groigno and Whitaker (1998) initiated chromosome disjunction and segregation in embryonic sea urchin cells by Ca^{2+} photorelease from NP-EGTA or by photolysis of caged IP3. Ca^{2+} buffers prevented chromatid separation but not the later stages of anaphase, indicating a specific role for Ca^{2+} in early anaphase chromosome disjunction. Tisa and Adler (1992) used electroporation to introduce Ca^{2+}-loaded nitr-5 or DM-nitrophen into *Escherichia coli* bacteria, and showed that elevation of $[Ca^{2+}]_i$ enhanced tumbling behavior characteristic of chemotaxis whereas photorelease of caged chelator from diazo-2 decreased tumbling. Photolysis of diazo-3, which reduces pH without affecting $[Ca^{2+}]_i$, caused only a small increase in tumbling. Mutants with methyl-accepting chemotaxis receptor proteins still responded to Ca^{2+}, whereas mutants of specific Che proteins did not, indicating that the action of these proteins lay downstream of the Ca^{2+} signal.

X. Conclusions

Interest in photolabile Ca^{2+} chelators has been intense. Their range of application has broadened well beyond the original nerve, muscle, and fibroblast preparations. They remain one of the most valuable tools for the precise definition of

calcium's roles and mechanisms of action in cell biology. They have attracted and challenged some of the best minds in physiology, resulting in great conceptual and skillful sophistication in the rapid evolution of this technology, which shows little sign of abating.

Acknowledgments

I thank Steve Adams for valuable discussion and Joseph Kao for drawings of chelator structures. The research done in my laboratory in this area was supported primarily by National Institutes of Health Grant NS 15114.

References

Adams, S. R., and Tsien, R. Y. (1993). Controlling cell chemistry with caged compounds. *Annu. Rev. Physiol.* **55,** 755–784.

Adams, S. R., Kao, J. P. Y., Grynkiewicz, G., Minta, A., and Tsien, R. Y. (1988). Biologically useful chelators that release Ca^{2+} upon illumination. *J. Am. Chem. Soc.* **110,** 3212–3220.

Adams, S. R., Kao, J. P. Y., and Tsien, R. Y. (1989). Biologically useful chelators that take up Ca^{2+} upon illumination. *J. Am. Chem. Soc.* **111,** 7957–7968.

Adams, S. R., Lev-Ram, V., and Tsien, R. Y. (1997). A new caged Ca^{2+}, azid-1, is far more photosensitive than nitrobenzyl-based chelators. *Chem. Biol.* **4,** 867–878.

Ashley, C. C., Griffiths, P. J., Lea, T. J., Mulligan, I. P., Palmer, R. E., and Simnett, S. J. (1991). Use of fluorescent TnC derivatives and ''caged'' compounds to study cellular Ca^{2+} phenomena. *In* ''Cellular Calcium: A Practical Approach,'' (J. G. McCormack, and P. H. Cobbold, eds.), pp. 177–203. Oxford University Press, New York.

Ashley, C. C., Mulligan, I. P., and Lea, T. J. (1991). Ca^{2+} and activation mechanisms in skeletal muscle. *Q. Rev. Biophys.* **24,** 1–73.

Ashley, C. C., Lea, T. J., Mulligan, I. P., Palmer, R. E., and Simnett, S. J. (1993). Activation and relaxation mechanisms in single muscle fibres. *Adv. Exp. Med. Biol.* **332,** 97–114.

Ayer, R. K., Jr., and Zucker, R. S. (1999). Magnesium binding to DM-nitrophen and its effect on the photorelease of calcium. *Biophys. J.* **77,** 3384–3393.

Backx, P. H., O'Rourke, B., and Marban, E. (1991). Flash photolysis of magnesium-DM-nitrophen in heart cells. A novel approach to probe magnesium- and ATP-dependent regulation of calcium channels. *Am. J. Hypertens.* **4,** 416S–421S.

Bates, S. E., and Gurney, A. M. (1993). Ca^{2+}-dependent block and potentiation of L-type calcium current in guinea-pig ventricular myocytes. *J. Physiol. (Lond.)* **466,** 345–365.

Bernardinelli, Y., Haeberli, C., and Chatton, J. Y. (2005). Flash photolysis using a light emitting diode: An efficient, compact, and affordable solution. *Cell Calcium* **37,** 565–572.

Beutner, D., Voets, T., Neher, E., and Moser, T. (2001). Calcium dependence of exocytosis and endocytosis at the cochlear inner hair cell afferent synapse. *Neuron* **29,** 681–690.

Bollmann, J. H., and Sakmann, B. (2005). Control of synaptic strength and timing by the release-site Ca^{2+} signal. *Nat. Neurosci.* **8,** 426–434.

Bollmann, J. H., Sakmann, B., and Borst, J. G. (2000). Calcium sensitivity of glutamate release in a calyx-type terminal. *Science* **289,** 953–957.

Brown, E. B., Shear, J. B., Adams, S. R., Tsien, R. Y., and Webb, W. W. (1999). Photolysis of caged calcium in femtoliter volumes using two-photon excitation. *Biophys. J.* **76,** 489–499.

Bruns, D., Engert, F., and Lux, H. D. (1993). A fast activating presynaptic reuptake current during serotonergic transmission in identified neurons of Hirudo. *Neuron* **10,** 559–572.

Buchet, R., Jona, I., and Martonosi, A. (1991). Ca^{2+} release from caged-Ca^{2+} alters the FTIR spectrum of sarcoplasmic reticulum. *Biochim. Biophys. Acta* **1069,** 209–217.

Buchet, R., Jona, I., and Martonosi, A. (1992). The effect of dicyclohexylcarbodiimide and cyclopiazonic acid on the difference FTIR spectra of sarcoplasmic reticulum induced by photolysis of caged-ATP and caged-Ca^{2+}. *Biochim. Biophys. Acta* **1104,** 207–214.

Carl, A., McHale, N. G., Publicover, N. G., and Sanders, K. M. (1990). Participation of Ca^{2+}-activated K^+ channels in electrical activity of canine gastric smooth muscle. *J. Physiol. (Lond.)* **429,** 205–221.

Cash, S., Dan, Y., Poo, M.-M., and Zucker, R. (1996). Postsynaptic elevation of calcium induces persistent depression of developing neuromuscular synapses. *Neuron* **16,** 745–754.

Cash, S., Zucker, R. S., and Poo, M.-M. (1996). Spread of synaptic depression mediated by presynaptic cytoplasmic signaling. *Science* **272,** 998–1001.

Charnet, P., Richard, S., Gurney, A. M., Ouadid, H., Tiaho, F., and Nargeot, J. (1991). Modulation of Ca currents in isolated frog atrial cells studied with photosensitive probes. Regulation by cAMP and Ca^{2+}: A common pathway? *J. Mol. Cell. Cardiol.* **23,** 343–356.

Delaney, K. R., and Zucker, R. S. (1990). Calcium released by photolysis of DM-nitrophen stimulates transmitter release at squid giant synapse. *J. Physiol. (Lond.)* **426,** 473–498.

DeLong, L. J., Phillips, C. M., Kaplan, J. H., Scarpa, A., and Blasie, J. K. (1990). A new method for monitoring the kinetics of calcium binding to the sarcoplasmic reticulum Ca^{2+}-ATPase employing the flash-photolysis of caged-calcium. *J. Biochem. Biophys. Methods* **21,** 333–339.

DelPrincipe, F., Egger, M., Ellis-Davies, G. C., and Niggli, E. (1999). Two-photon and UV-laser flash photolysis of the Ca^{2+} cage, dimethoxynitrophenyl-EGTA-4. *Cell Calcium* **25,** 85–91.

Denk, W. (1997). Pulsing mercury arc lamps for uncaging and fast imaging. *J. Neurosci. Methods* **72,** 39–42.

Denk, W., Strickler, J. H., and Webb, W. W. (1990). Two-photon laser scanning fluorescence microscopy. *Science* **248,** 73–76.

Duncan, G., Rabl, K., Gemp, I., Heidelberger, R., and Thoreson, W. B. (2010). Quantitative analysis of synaptic release at the photoreceptor synapse. *Biophys. J.* **98,** 2102–2110.

Eberhard, M., and Erne, P. (1991). Calcium binding to fluorescent calcium indicators: Calcium green, calcium orange and calcium crimson. *Biochem. Biophys. Res. Commun.* **180,** 209–215.

Eberius, C., and Schild, D. (2001). Local photolysis using tapered quartz fibres. *Pflügers Arch.* **443,** 323–330.

Ellis-Davies, G. C. (2003). Development and application of caged calcium. *Methods Enzymol.* **360,** 226–238.

Ellis-Davies, G. C. (2006). DM-nitrophen AM is caged magnesium. *Cell Calcium* **39,** 471–473.

Ellis-Davies, G. C., and Barsotti, R. J. (2006). Tuning caged calcium: Photolabile analogues of EGTA with improved optical and chelation properties. *Cell Calcium* **39,** 75–83.

Ellis-Davies, G. C. R., and Kaplan, J. H. (1988). A new class of photolabile chelators for the rapid release of divalent cations: Generation of caged Ca and caged Mg. *J. Org. Chem.* **53,** 1966–1969.

Ellis-Davies, G. C., and Kaplan, J. H. (1994). Nitrophenyl-EGTA, a photolabile chelator that selectively binds Ca^{2+} with high affinity and releases it rapidly upon photolysis. *Proc. Natl. Acad. Sci. USA* **91,** 187–191.

Ellis-Davies, G. C., Kaplan, J. H., and Barsotti, R. J. (1996). Laser photolysis of caged calcium: Rates of calcium release by nitrophenyl-EGTA and DM-nitrophen. *Biophys. J.* **70,** 1006–1016.

Engert, F., Paulus, G. G., and Bonhoeffer, T. (1996). A low-cost UV laser for flash photolysis of caged compounds. *J. Neurosci. Methods* **66,** 47–54.

Escobar, A. L., Cifuentes, F., and Vergara, J. L. (1995). Detection of Ca^{2+}-transients elicited by flash photolysis of DM-nitrophen with a fast calcium indicator. *FEBS Lett.* **364,** 335–338.

Escobar, A. L., Vélez, P., Kim, A. M., Cifuentes, F., Fill, M., and Vergara, J. L. (1997). Kinetic properties of DM-nitrophen and calcium indicators: Rapid transient response to flash photolysis. *Pflügers Arch.* **434,** 615–631.

Faas, G. C., Karacs, K., Vergara, J. L., and Mody, I. (2005). Kinetic properties of DM-nitrophen binding to calcium and magnesium. *Biophys. J.* **88,** 4421–4433.

Faas, G. C., Schwaller, B., Vergara, J. L., and Mody, I. (2007). Resolving the fast kinetics of cooperative binding: Ca^{2+} buffering by calretinin. *PLoS Biol.* **5,** e311.

Felmy, F., Neher, E., and Schneggenburger, R. (2003). Probing the intracellular calcium sensitivity of transmitter release during synaptic facilitation. *Neuron* **37,** 801–811.

Felmy, F., Neher, E., and Schneggenburger, R. (2003). The timing of phasic transmitter release is Ca^{2+}-dependent and lacks a direct influence of presynaptic membrane potential. *Proc. Natl. Acad. Sci. USA* **100,** 15200–15205.

Ferenczi, M. A., Goldman, Y. E., and Trentham, D. R. (1989). Relaxation of permeabilized, isolated muscle-fibers of the rabbit by rapid chelation of Ca-$^{2+}$-ions through laser-pulse photolysis of caged-Bapta. *J. Physiol. (Lond.)* **418,** P155.

Fischer, T. M., Zucker, R. S., and Carew, T. J. (1997). Activity-dependent potentiation of synaptic transmission from L30 inhibitory interneurons of aplysia depends on residual presynaptic Ca^{2+} but not on postsynaptic Ca^{2+}. *J. Neurophysiol.* **78,** 2061–2071.

Fleet, A., Ellis-Davies, G., and Bolsover, S. (1998). Calcium buffering capacity of neuronal cell cytosol measured by flash photolysis of calcium buffer NP-EGTA. *Biochem. Biophys. Res. Commun.* **250,** 786–790.

Fogelson, A. L., and Zucker, R. S. (1985). Presynaptic calcium diffusion from various arrays of single channels. Implications for transmitter release and synaptic facilitation. *Biophys. J.* **48,** 1003–1017.

Forbush, B., 3rd, and Klodos, I. (1991). Rate-limiting steps in Na translocation by the Na/K pump. *Soc. Gen. Physiol. Ser.* **46,** 210–225.

Fricker, M. D., Gilroy, S., Read, N. D., and Trewavas, A. J. (1991). Visualisation and measurement of the calcium message in guard cells. *Symp. Soc. Exp. Biol.* **45,** 177–190.

Fryer, M. W., and Zucker, R. S. (1993). Ca^{2+}-dependent inactivation of Ca^{2+} current in Aplysia neurons: Kinetic studies using photolabile Ca^{2+} chelators. *J. Physiol. (Lond.)* **464,** 501–528.

Gilroy, S., Fricker, M. D., Read, N. D., and Trewavas, A. J. (1991). Role of calcium in signal transduction of *Commelina* guard cells. *Plant Cell* **3,** 333–344.

Godwin, D. W., Che, D., O'Malley, D. M., and Zhou, Q. (1997). Photostimulation with caged neurotransmitters using fiber optic lightguides. *J. Neurosci. Methods* **73,** 91–106.

Goldman, Y. E., Hibberd, M. G., and Trentham, D. R. (1984). Relaxation of rabbit psoas muscle fibres from rigor by photochemical generation of adenosine-5′-triphosphate. *J. Physiol. (Lond.)* **354,** 577–604.

Grell, E., Lewitzki, E., Ruf, H., Bamberg, E., Ellis-Davies, G. C., Kaplan, J. H., and de Weer, P. (1989). Caged-Ca^{2+}: A new agent allowing liberation of free Ca^{2+} in biological systems by photolysis. *Cell. Mol. Biol.* **35,** 515–522.

Groigno, L., and Whitaker, M. (1998). An anaphase calcium signal controls chromosome disjunction in early sea urchin embryos. *Cell* **92,** 193–204.

Grynkiewicz, G., Poenie, M., and Tsien, R. Y. (1985). A new generation of Ca^{2+} indicators with greatly improved fluorescence properties. *J. Biol. Chem.* **260,** 3440–3450.

Gurney, A. (1991). Photolabile calcium buffers to selectively activate calcium-dependent processes. *In* "Cellular Neurobiology: A Practical Approach," (J. Chad, and H. Wheal, eds.), pp. 153–177. IRL Press, New York.

Gurney, A. (1993). Photolabile caged compounds. *In* "Fluorescent and Luminescent Probes for Biological Activity—A Practical Guide to Technology for Quantitative Real-Time Analysis," (W. T. Mason, ed.), pp. 335–348. Academic Press, San Diego.

Gurney, A. M., Tsien, R. Y., and Lester, H. A. (1987). Activation of a potassium current by rapid photochemically generated step increases of intracellular calcium in rat sympathetic neurons. *Proc. Natl. Acad. Sci. USA* **84,** 3496–3500.

Gurney, A. M., Charnet, P., Pye, J. M., and Nargeot, J. (1989). Augmentation of cardiac calcium current by flash photolysis of intracellular caged-Ca^{2+} molecules. *Nature* **341,** 65–68.

Györke, S., and Fill, M. (1993). Ryanodine receptor adaptation: Control mechanism of Ca^{2+}-induced Ca^{2+} release in heart. *Science* **260,** 807–809.

Hadley, R. W., and Lederer, W. J. (1991). Ca^{2+} and voltage inactivate Ca^{2+} channels in guinea-pig ventricular myocytes through independent mechanisms. *J. Physiol. (Lond.)* **444,** 257–268.

Hadley, R. W., Kirby, M. S., Lederer, W. J., and Kao, J. P. (1993). Does the use of DM-nitrophen, nitr-5, or diazo-2 interfere with the measurement of indo-1 fluorescence? *Biophys. J.* **65,** 2537–2546.

Harootunian, A. T., Kao, J. P., and Tsien, R. Y. (1988). Agonist-induced calcium oscillations in depolarized fibroblasts and their manipulation by photoreleased Ins(1, 4, 5)P3, Ca++, and Ca++ buffer. *Cold Spring Harb. Symp. Quant. Biol.* **53**(Pt. 2), 935–943.

Harootunian, A. T., Kao, J. P., Paranjape, S., Adams, S. R., Potter, B. V., and Tsien, R. Y. (1991). Cytosolic Ca^{2+} oscillations in REF52 fibroblasts: Ca^{2+}-stimulated IP3 production or voltage-dependent Ca^{2+} channels as key positive feedback elements. *Cell Calcium* **12,** 153–164.

Haydon, P. G., Man-Son-Hing, H., Doyle, R. T., and Zoran, M. (1991). FMRFamide modulation of secretory machinery underlying presynaptic inhibition of synaptic transmission requires a pertussis toxin-sensitive G-protein. *J. Neurosci.* **11,** 3851–3860.

Heidelberger, R., Heinemann, C., Neher, E., and Matthews, G. (1994). Calcium dependence of the rate of exocytosis in a synaptic terminal. *Nature* **371,** 513–515.

Heinemann, C., Chow, R. H., Neher, E., and Zucker, R. S. (1994). Kinetics of the secretory response in bovine chromaffin cells following flash photolysis of caged Ca^{2+}. *Biophys. J.* **67,** 2546–2557.

Hochner, B., Parnas, H., and Parnas, I. (1989). Membrane depolarization evokes neurotransmitter release in the absence of calcium entry. *Nature* **342,** 433–435.

Hosoi, N., Sakaba, T., and Neher, E. (2007). Quantitative analysis of calcium-dependent vesicle recruitment and its functional role at the calyx of Held synapse. *J. Neurosci.* **27,** 14286–14298.

Hsu, S. F., Augustine, G. J., and Jackson, M. B. (1996). Adaptation of Ca^{2+}-triggered exocytosis in presynaptic terminals. *Neuron* **17,** 501–512.

Iino, M., and Endo, M. (1992). Calcium-dependent immediate feedback control of inositol 1,4,5-triphosphate-induced Ca^{2+} release. *Nature* **360,** 76–78.

Johnson, B. D., and Byerly, L. (1993). Photo-released intracellular Ca^{2+} rapidly blocks Ba^{2+} current in *Lymnaea* neurons. *J. Physiol. (Lond.)* **462,** 321–347.

Kamiya, H., and Zucker, R. S. (1994). Residual Ca^{2+} and short-term synaptic plasticity. *Nature* **371,** 603–606.

Kao, J. P., and Adams, S. R. (1993). Photosensitive caged compounds: Design, properties, and biological applications. *In* "Optical Microscopy: New Technologies and Applications," (B. Herman, and J. J. Lemasters, eds.), pp. 27–85. Academic Press, New York.

Kao, J. P., Harootunian, A. T., and Tsien, R. Y. (1989). Photochemically generated cytosolic calcium pulses and their detection by fluo-3. *J. Biol. Chem.* **264,** 8179–8184.

Kao, J. P., Alderton, J. M., Tsien, R. Y., and Steinhardt, R. A. (1990). Active involvement of Ca^{2+} in mitotic progression of Swiss 3T3 fibroblasts. *J. Cell Biol.* **111,** 183–196.

Kaplan, J. H. (1990). Photochemical manipulation of divalent cation levels. *Annu. Rev. Physiol.* **52,** 897–914.

Kaplan, J. H., and Ellis-Davies, G. C. (1988). Photolabile chelators for the rapid photorelease of divalent cations. *Proc. Natl. Acad. Sci. USA* **85,** 6571–6575.

Kaplan, J. H., and Somlyo, A. P. (1989). Flash photolysis of caged compounds: New tools for cellular physiology. *Trends Neurosci.* **12,** 54–59.

Kaplan, J. H., Forbush, B., 3rd, and Hoffman, J. F. (1978). Rapid photolytic release of adenosine 5′-triphosphate from a protected analogue: Utilization by the Na:K pump of human red blood cell ghosts. *Biochemistry* **17,** 1929–1935.

Kasai, H., Kishimoto, T., Liu, T. T., Miyashita, Y., Podini, P., Grohovaz, F., and Meldolesi, J. (1999). Multiple and diverse forms of regulated exocytosis in wild-type and defective PC12 cells. *Proc. Natl. Acad. Sci. USA* **96,** 945–949.

Kasono, K., and Hirano, T. (1994). Critical role of postsynaptic calcium in cerebellar long-term depression. *Neuroreport* **6,** 17–20.

Kentish, J. C., Barsotti, R. J., Lea, T. J., Mulligan, I. P., Patel, J. R., and Ferenczi, M. A. (1990). Calcium release from cardiac sarcoplasmic reticulum induced by photorelease of calcium or Ins(1, 4, 5)P3. *Am. J. Physiol.* **258,** H610–H615.

Kimitsuki, T., and Ohmori, H. (1992). The effect of caged calcium release on the adaptation of the transduction current in chick hair cells. *J. Physiol. (Lond.)* **458,** 27–40.

Konishi, M., Hollingworth, S., Harkins, A. B., and Baylor, S. M. (1991). Myoplasmic calcium transients in intact frog skeletal muscle fibers monitored with the fluorescent indicator furaptra. *J. Gen. Physiol.* **97,** 271–301.

Kurebayashi, N., Harkins, A. B., and Baylor, S. M. (1993). Use of fura red as an intracellular calcium indicator in frog skeletal muscle fibers. *Biophys. J.* **64,** 1934–1960.

Lancaster, B., and Zucker, R. S. (1994). Photolytic manipulation of Ca^{2+} and the time course of slow, Ca^{2+}-activated K^+ current in rat hippocampal neurones. *J. Physiol. (Lond.)* **475,** 229–239.

Landò, L., and Zucker, R. S. (1989). "Caged calcium" in *Aplysia* pacemaker neurons. Characterization of calcium-activated potassium and nonspecific cation currents. *J. Gen. Physiol.* **93,** 1017–1060.

Landò, L., and Zucker, R. S. (1994). Ca^{2+} cooperativity in neurosecretion measured using photolabile Ca^{2+} chelators. *J. Neurophysiol.* **72,** 825–830.

Lannergren, J., and Arner, A. (1992). Relaxation rate of intact striated muscle fibres after flash photolysis of a caged calcium chelator (diazo-2). *J. Muscle Res. Cell Motil.* **13,** 630–634.

Lau, P. M., Zucker, R. S., and Bentley, D. (1999). Induction of filopodia by direct local elevation of intracellular calcium ion concentration. *J. Cell Biol.* **145,** 1265–1275.

Lea, T. J., and Ashley, C. C. (1990). Ca^{2+} release from the sarcoplasmic reticulum of barnacle myofibrillar bundles initiated by photolysis of caged Ca^{2+}. *J. Physiol. (Lond.)* **427,** 435–453.

Lev-Ram, V., Jiang, T., Wood, J., Lawrence, D. S., and Tsien, R. Y. (1997). Synergies and coincidence requirements between NO, cGMP, and Ca^{2+} in the induction of cerebellar long-term depression. *Neuron* **18,** 1025–1038.

Malenka, R. C., Kauer, J. A., Zucker, R. S., and Nicoll, R. A. (1988). Postsynaptic calcium is sufficient for potentiation of hippocampal synaptic transmission. *Science* **242,** 81–84.

Malenka, R. C., Lancaster, B., and Zucker, R. S. (1992). Temporal limits on the rise in postsynaptic calcium required for the induction of long-term potentiation. *Neuron* **9,** 121–128.

Man-Son-Hing, H., Zoran, M. J., Lukowiak, K., and Haydon, P. G. (1989). A neuromodulator of synaptic transmission acts on the secretory apparatus as well as on ion channels. *Nature* **341,** 237–239.

Marrion, N. V., Zucker, R. S., Marsh, S. J., and Adams, P. R. (1991). Modulation of M-current by intracellular Ca^{2+}. *Neuron* **6,** 533–545.

Matveev, V., Sherman, A., and Zucker, R. S. (2002). New and corrected simulations of synaptic facilitation. *Biophys. J.* **83,** 1368–1373.

Matveev, V., Zucker, R. S., and Sherman, A. (2004). Facilitation through buffer saturation: Constraints on endogenous buffering properties. *Biophys. J.* **86,** 2691–2709.

Matveev, V., Bertram, R., and Sherman, A. (2006). Residual bound Ca^{2+} can account for the effects of Ca^{2+} buffers on synaptic facilitation. *J. Neurophysiol.* **96,** 3389–3397.

Matveev, V., Bertram, R., and Sherman, A. (2009). Ca^{2+} current versus Ca^{2+} channel cooperativity of exocytosis. *J. Neurosci.* **29,** 12196–12209.

McCray, J. A., and Trentham, D. R. (1989). Properties and uses of photoreactive caged compounds. *Annu. Rev. Biophys. Biophys. Chem.* **18,** 239–270.

McCray, J. A., Fidler-Lim, N., Ellis-Davies, G. C., and Kaplan, J. H. (1992). Rate of release of Ca^{2+} following laser photolysis of the DM-nitrophen-Ca^{2+} complex. *Biochemistry* **31,** 8856–8861.

Millar, A. G., Zucker, R. S., Ellis-Davies, G. C., Charlton, M. P., and Atwood, H. L. (2005). Calcium sensitivity of neurotransmitter release differs at phasic and tonic synapses. *J. Neurosci.* **25,** 3113–3125.

Minta, A., and Tsien, R. Y. (1989). Fluorescent indicators for cytosolic sodium. *J. Biol. Chem.* **264,** 19449–19457.

Momotake, A., Lindegger, N., Niggli, E., Barsotti, R. J., and Ellis-Davies, G. C. (2006). The nitrodibenzofuran chromophore: A new caging group for ultra-efficient photolysis in living cells. *Nat. Methods* **3,** 35–40.

Morad, M., Davies, N. W., Kaplan, J. H., and Lux, H. D. (1988). Inactivation and block of calcium channels by photo-released Ca^{2+} in dorsal root ganglion neurons. *Science* **241,** 842–844.

Mulkey, R. M., and Zucker, R. S. (1991). Action potentials must admit calcium to evoke transmitter release. *Nature* **350,** 153–155.

Mulkey, R. M., and Zucker, R. S. (1993). Calcium released by photolysis of DM-nitrophen triggers transmitter release at the crayfish neuromuscular junction. *J. Physiol. (Lond.)* **462,** 243–260.

Mulligan, I. P., and Ashley, C. C. (1989). Rapid relaxation of single frog skeletal muscle fibres following laser flash photolysis of the caged calcium chelator, diazo-2. *FEBS Lett.* **255,** 196–200.

Näbauer, M., and Morad, M. (1990). Ca^{2+}-induced Ca^{2+} release as examined by photolysis of caged Ca^{2+} in single ventricular myocytes. *Am. J. Physiol.* **258,** C189–C193.

Näbauer, M., Ellis-Davies, G. C., Kaplan, J. H., and Morad, M. (1989). Modulation of Ca^{2+} channel selectivity and cardiac contraction by photorelease of Ca^{2+}. *Am. J. Physiol.* **256,** H916–H920.

Nägerl, U. V., Novo, D., Mody, I., and Vergara, J. L. (2000). Binding kinetics of calbindin-D(28k) determined by flash photolysis of caged Ca^{2+}. *Biophys. J.* **79,** 3009–3018.

Naraghi, M., Muller, T. H., and Neher, E. (1998). Two-dimensional determination of the cellular Ca^{2+} binding in bovine chromaffin cells. *Biophys. J.* **75,** 1635–1647.

Neher, E., and Zucker, R. S. (1993). Multiple calcium-dependent processes related to secretion in bovine chromaffin cells. *Neuron* **10,** 21–30.

Neveu, D., and Zucker, R. S. (1996). Long-lasting potentiation and depression without presynaptic activity. *J. Neurophysiol.* **75,** 2157–2160.

Neveu, D., and Zucker, R. S. (1996). Postsynaptic levels of $[Ca^{2+}]_i$ needed to trigger LTD and LTP. *Neuron* **16,** 619–629.

Nowycky, M. C., and Pinter, M. J. (1993). Time courses of calcium and calcium-bound buffers following calcium influx in a model cell. *Biophys. J.* **64,** 77–91.

O'Neill, S. C., Mill, J. G., and Eisner, D. A. (1990). Local activation of contraction in isolated rat ventricular myocytes. *Am. J. Physiol.* **258,** C1165–C1168.

O'Rourke, B., Backx, P. H., and Marban, E. (1992). Phosphorylation-independent modulation of L-type calcium channels by magnesium-nucleotide complexes. *Science* **257,** 245–248.

Ogden, D. (1988). Cell physiology. Answer in a flash. *Nature* **336,** 16–17.

Ogden, D. C., Capiod, T., Walker, J. W., and Trentham, D. R. (1990). Kinetics of the conductance evoked by noradrenaline, inositol trisphosphate or Ca^{2+} in guinea-pig isolated hepatocytes. *J. Physiol. (Lond.)* **422,** 585–602.

Ohnuma, K., Whim, M. D., Fetter, R. D., Kaczmarek, L. K., and Zucker, R. S. (2001). Presynaptic target of Ca^{2+} action on neuropeptide and acetylcholine release in *Aplysia californica*. *J. Physiol. (Lond.)* **535,** 647–662.

Palmer, R. E., Mulligan, I. P., Nunn, C., and Ashley, C. C. (1990). Striated scallop muscle relaxation: Fast force transients produced by photolysis of Diazo-2. *Biochem. Biophys. Res. Commun.* **168,** 295–300.

Palmer, R. E., Simnett, S. J., Mulligan, I. P., and Ashley, C. C. (1991). Skeletal muscle relaxation with diazo-2: The effect of altered pH. *Biochem. Biophys. Res. Commun.* **181,** 1337–1342.

Pan, B., and Zucker, R. S. (2009). A general model of synaptic transmission and short-term plasticity. *Neuron* **62,** 539–554.

Parker, I. (1992). Caged intracellular messengers and the inositol phosphate signaling pathway. *In* "Intracellular Messengers. Neuromethods Vol. 20," (A. A. Boulton, G. B. Baker, and C. W. Taylor, eds.), pp. 369–396. Humana Press, Totowa, NJ.

Parsons, T. D., Ellis-Davies, G. C., and Almers, W. (1996). Millisecond studies of calcium-dependent exocytosis in pituitary melanotrophs: Comparison of the photolabile calcium chelators nitrophenyl-EGTA and DM-nitrophen. *Cell Calcium* **19,** 185–192.

Rapp, G., and Guth, K. (1988). A low cost high intensity flash device for photolysis experiments. *Pflügers Arch.* **411,** 200–203.

Rebrik, T. I., Kotelnikova, E. A., and Korenbrot, J. I. (2000). Time course and Ca^{2+} dependence of sensitivity modulation in cyclic GMP-gated currents of intact cone photoreceptors. *J. Gen. Physiol.* **116,** 521–534.

Sah, P., and Clements, J. D. (1999). Photolytic manipulation of $[Ca^{2+}]_i$ reveals slow kinetics of potassium channels underlying the after hyperpolarization in hippocampal pyramidal neurons. *J. Neurosci.* **19,** 3657–3664.

Sakaba, T., Stein, A., Jahn, R., and Neher, E. (2005). Distinct kinetic changes in neurotransmitter release after SNARE protein cleavage. *Science* **309,** 491–494.

Sala, F., and Hernández-Cruz, A. (1990). Calcium diffusion modeling in a spherical neuron. Relevance of buffering properties. *Biophys. J.* **57,** 313–324.

Scarpa, A., Brinley, F. J., Jr., Tiffert, T., and Dubyak, G. R. (1978). Metallochromic indicators of ionized calcium. *Ann. NY Acad. Sci.* **307,** 86–112.

Schneggenburger, R., and Neher, E. (2000). Intracellular calcium dependence of transmitter release rates at a fast central synapse. *Nature* **406,** 889–893.

Simon, S. M., and Llinás, R. R. (1985). Compartmentalization of the submembrane calcium activity during calcium influx and its significance in transmitter release. *Biophys. J.* **48,** 485–498.

Stern, M. D. (1992). Buffering of calcium in the vicinity of a channel pore. *Cell Calcium* **13,** 183–192.

Stockbridge, N., and Moore, J. W. (1984). Dynamics of intracellular calcium and its possible relationship to phasic transmitter release and facilitation at the frog neuromuscular junction. *J. Neurosci.* **4,** 803–811.

Tanaka, K., Khiroug, L., Santamaria, F., Doi, T., Ogasawara, H., Ellis-Davies, G. C., Kawato, M., and Augustine, G. J. (2007). Ca^{2+} requirements for cerebellar long-term synaptic depression: role for a postsynaptic leaky integrator. *Neuron* **54,** 787–800.

Tang, Y., and Zucker, R. S. (1997). Mitochondrial involvement in post-tetanic potentiation of synaptic transmission. *Neuron* **18,** 483–491.

Tang, Y., Schlumpberger, T., Kim, T., Lueker, M., and Zucker, R. S. (2000). Effects of mobile buffers on facilitation: Experimental and computational studies. *Biophys. J.* **78,** 2735–2751.

Thomas, P., Wong, J. G., and Almers, W. (1993). Millisecond studies of secretion in single rat pituitary cells stimulated by flash photolysis of caged Ca^{2+}. *EMBO J.* **12,** 303–306.

Tisa, L. S., and Adler, J. (1992). Calcium ions are involved in *Escherichia coli* chemotaxis. *Proc. Natl. Acad. Sci. USA* **89,** 11804–11808.

Tsien, R. Y., and Zucker, R. S. (1986). Control of cytoplasmic calcium with photolabile tetracarboxylate 2-nitrobenzhydrol chelators. *Biophys. J.* **50,** 843–853.

Valdeolmillos, M., O'Neill, S. C., Smith, G. L., and Eisner, D. A. (1989). Calcium-induced calcium release activates contraction in intact cardiac cells. *Pflügers Arch.* **413,** 676–678.

Vélez, P., Gyorke, S., Escobar, A. L., Vergara, J., and Fill, M. (1997). Adaptation of single cardiac ryanodine receptor channels. *Biophys. J.* **72,** 691–697.

Wadel, K., Neher, E., and Sakaba, T. (2007). The coupling between synaptic vesicles and Ca^{2+} channels determines fast neurotransmitter release. *Neuron* **53,** 563–575.

Walker, J. W. (1991). Caged molecules activated by light. *In* "Cellular Neurobiology: A Practical Approach," (J. Chad, and H. Wheal, eds.), pp. 179–203. IRL Press, New York.

Wang, S. S., and Augustine, G. J. (1995). Confocal imaging and local photolysis of caged compounds: Dual probes of synaptic function. *Neuron* **15,** 755–760.

Wang, J., and Zucker, R. S. (2001). Photolysis-induced suppression of inhibition in rat hippocampal CA1 pyramidal neurons. *J. Physiol. (Lond.)* **533,** 757–763.

Wang, J., Yeckel, M. F., Johnston, D., and Zucker, R. S. (2004). Photolysis of postsynaptic caged Ca^{2+} can potentiate and depress mossy fiber synaptic responses in rat hippocampal CA3 pyramidal neurons. *J. Neurophysiol.* **91,** 1596–1607.

Xu, T., Naraghi, M., Kang, H., and Neher, E. (1997). Kinetic studies of Ca^{2+} binding and Ca^{2+} clearance in the cytosol of adrenal chromaffin cells. *Biophys. J.* **73,** 532–545.

Yamada, W. M., and Zucker, R. S. (1992). Time course of transmitter release calculated from simulations of a calcium diffusion model. *Biophys. J.* **61,** 671–682.

Yang, S. N., Tang, Y. G., and Zucker, R. S. (1999). Selective induction of LTP and LTD by postsynaptic $[Ca^{2+}]_i$ elevation. *J. Neurophysiol.* **81,** 781–787.

Young, S. M., Jr., and Neher, E. (2009). Synaptotagmin has an essential function in synaptic vesicle positioning for synchronous release in addition to its role as a calcium sensor. *Neuron* **63,** 482–496.

Zoran, M. J., Doyle, R. T., and Haydon, P. G. (1991). Target contact regulates the calcium responsiveness of the secretory machinery during synaptogenesis. *Neuron* **6,** 145–151.

Zucker, R. S. (1989). Models of calcium regulation in neurons. *In* "Neural Models of Plasticity: Experimental and Theoretical Approaches," (J. H. Byrne, and W. O. Berry, eds.), pp. 403–422. Academic Press, Orlando, FL.

Zucker, R. S. (1992). Effects of photolabile calcium chelators on fluorescent calcium indicators. *Cell Calcium* **13,** 29–40.

Zucker, R. S. (1993). The calcium concentration clamp: Spikes and reversible pulses using the photolabile chelator DM-nitrophen. *Cell Calcium* **14,** 87–100.

Zucker, R. S., and Haydon, P. G. (1988). Membrane potential has no direct role in evoking neurotransmitter release. *Nature* **335,** 360–362.

Zucker, R. S., and Stockbridge, N. (1983). Presynaptic calcium diffusion and the time courses of transmitter release and synaptic facilitation at the squid giant synapse. *J. Neurosci.* **3,** 1263–1269.